

SYNTHESIS AND CHARACTERISATION OF ELECTROCERAMICS

NEOH SHIAO SUANG

**A project report submitted in partial fulfilment of the
requirements for the award of the degree of
Bachelor (Hons.) of Material and Manufacturing Engineering**

**Faculty of Engineering and Science
Universiti Tunku Abdul Rahman**

April 2011

DECLARATION

I hereby declare that this project report is based on my original work except for citations and quotations which have been duly acknowledged. I also declare that it has not been previously and concurrently submitted for any other degree or award at UTAR or other institutions.

Signature : _____

Name : _____

ID No. : _____

Date : _____

APPROVAL FOR SUBMISSION

I certify that this project report entitled **“SYNTHESIS AND CHARACTERISATION OF ELECTROCERAMICS”** was prepared by **NEOH SHIAO SUANG** has met the required standard for submission in partial fulfilment of the requirements for the award of Bachelor of Engineering (Hons.) Material and Manufacturing Engineering at Universiti Tunku Abdul Rahman.

Approved by,

Signature : _____

Supervisor: Assistant Prof. Dr. Khaw Chwin Chieh

Date : _____

The copyright of this report belongs to the author under the terms of the copyright Act 1987 as qualified by Intellectual Property Policy of Universiti Tunku Abdul Rahman. Due acknowledgement shall always be made of the use of any material contained in, or derived from, this report.

© 2011, Neoh Shiao Suang. All right reserved.

SYNTHESIS AND CHARACTERISATION OF ELECTROCERAMICS

ABSTRACT

Phase purity of $\text{Sr}_{1-x}\text{Bi}_{2+2x/3}\text{Ta}_2\text{O}_9$ ($x= 0, 0.1, 0.2, 0.3$) prepared by conventional solid state method were investigated by X-Ray Diffraction (XRD) method. For $x=0.2$ and 0.3 , the samples failed to obtain a single homogeneous phase since the single phase material only can be achieved when $x<0.15$. However, in this a tiny BiTaO_4 peak were observed at distributed $\sim 30^\circ$ in the samples of $x=0.0$ and $x=0.1$ synthesized at 1100°C ; at 1200°C , the samples were partially melted. Sample prepared by ball milling method, $\text{Sr}_{1-x}\text{Bi}_{2+2x/3}\text{Ta}_2\text{O}_9$ ($x= 0$ and 0.3) failed to produce single phase because of the limited milling time (4 hours). Few impurity phases were observed in those samples. Impedance studies were carried out on selected samples. From the Cole-cole plots ($Z''-Z'$), all samples exhibited two overlapping semicircle corresponding to grain and grain boundary. $\text{SrBi}_2\text{Ta}_2\text{O}_9$ and $\text{Sr}_{0.9}\text{Bi}_{2.1}\text{Ta}_2\text{O}_9$ prepared by conventional solid state method were electrically homogeneous while $\text{SrBi}_2\text{Ta}_2\text{O}_9$ prepared by ball milling process was electrically heterogeneous probably because of the limited milling time. Permittivity of $\text{SrBi}_2\text{Ta}_2\text{O}_9$ at room temperature is 221 and 275 for conventional solid-state and ball milling method, respectively. The values are comparable to the reported value in the literature (260). On the other hand, for $\tan \delta$, $\text{SrBi}_2\text{Ta}_2\text{O}_9$ at room temperature is 0.002 and 0.014 for conventional solid-state and ball milling method, respectively. The values are comparable to the reported value in the literature (0.08) Ball milling method tends to enhance property of sample and thus leads to higher values in those regions. Activation energy of three samples was in the range of 1.019 to 1.315 eV is good agreement with the reported value in the literature.

TABLE OF CONTENTS

DECLARATION		ii
APPROVAL FOR SUBMISSION		iii
ABSTRACT		v
TABLE OF CONTENTS		vi
LIST OF TABLES		viii
LIST OF FIGURES		ix
LIST OF SYMBOLS / ABBREVIATIONS		xii
 CHAPTER		
1	INTRODUCTION	1
	1.1 Background	1
	1.2 Objective	5
 2	 LITERATURE REVIEW	 6
	2.1 $\text{Sr}_2\text{Bi}_2\text{Ta}_2\text{O}_9$	6
	2.2 $\text{Sr}_{0.8}\text{Bi}_2\text{Ta}_2\text{O}_9$	11
	2.3 Non-stoichiometric $\text{Sr}_{1-x}\text{Bi}_{2+2x/3}\text{Ta}_2\text{O}_9$ ceramics	12
	2.4 Strontium Bismuth Niobate (SBN)	13
 3	 METHODOLOGY	 16
	3.1 Introduction	16
	3.2 Sample Preparation	18

3.3	Characterisation	19
3.3.1	XRD	19
3.3.2	Impedance Studies	19
3.4	Flow Chart	20
3.5	Gann Chart	22
4	Result and Discussion	23
4.1	XRD Analysis	23
4.1.1	Phase Formation Study of $\text{SrBi}_2\text{Ta}_2\text{O}_9$ (Solid-state Method)	26
4.1.2	Phase Formation Study of $\text{SrBi}_2\text{Ta}_2\text{O}_9$ (Ball Milling)	27
4.1.3	Phase Formation Study of $\text{Sr}_{0.9}\text{Bi}_{2.1}\text{Ta}_2\text{O}_9$ (Solid-state Method)	28
4.1.4	Phase Formation Study of $\text{Sr}_{0.8}\text{Bi}_{2.4}\text{Ta}_2\text{O}_9$ (Solid-state Method)	30
4.1.5	Phase Formation Study of $\text{Sr}_{0.7}\text{Bi}_{2.2}\text{Ta}_2\text{O}_9$ (Solid-state Method)	31
4.1.6	Phase Formation Study of $\text{Sr}_{0.7}\text{Bi}_{2.2}\text{Ta}_2\text{O}_9$ (Ball Milling)	32
4.2	Electrical Properties	33
4.2.1	Complex Impedance Study	33
4.2.2	Permittivity and Dielectric Loss Studies	41
4.2.3	Conductivity	42
5	Conclusion and Recommendations	46
5.1	Conclusion	46
5.2	Recommendation	47
	References	48
	Appendices	51

LIST OF TABLES

TABLE	TITLE	PAGE
4-1	Capacitance of $\text{SrBi}_2\text{Ta}_2\text{O}_9$ measured at 700 °C at 10 kHz	34
4-2	ϵ' of $\text{Sr}_{1-x}\text{Bi}_{2+2x/3}\text{Ta}_2\text{O}_9$ (x=0, 0.1) material measured at 10 kHz	41
4-3	$\tan \delta$ of $\text{Sr}_{1-x}\text{Bi}_{2+2x/3}\text{Ta}_2\text{O}_9$ (x=0, 0.1) material measured at 10 kHz	42
4-4	Conductivity and activation energy of grain and grain boundary phases.	43

LIST OF FIGURES

FIGURE	TITLE	PAGE
3-1	Flow chart for sample preparation using Conventional solid state sintering method And characterisation	18
3-2	Flow chart for sample preparation using solid State sintering method with ball milling and Characterisation	19
3-3	Gantt chart for the project	22
4-1	X-Ray diffraction patterns of $\text{Sr}_{1-x}\text{Bi}_{2+2x/3}\text{Ta}_2\text{O}_9$ ceramics (a) $x=0.3$ (b) $x=0.2$ (c) $x=0.1$ and (d) $x=0$ Prepared by conventional solid state method	24
4-2	X-Ray diffraction patterns of $\text{Sr}_{1-x}\text{Bi}_{2+2x/3}\text{Ta}_2\text{O}_9$ ceramics (a) $x=0.3$ and (b) $x=0$ prepared by ball milling process	25
4-3	X-ray diffraction patterns of $\text{SrBi}_2\text{Ta}_2\text{O}_9$ (solid-state) synthesized at a) $1000\text{ }^\circ\text{C}$ for 2 hours b) $1000\text{ }^\circ\text{C}$ for 4 hours and c) $1100\text{ }^\circ\text{C}$ for 4 hours	26
4-4	XRD patterns of $\text{SrBi}_2\text{Ta}_2\text{O}_9$ (ball milled) synthesis at (a) $650\text{ }^\circ\text{C}$ for 2 hours, (b) $650\text{ }^\circ\text{C}$ for 4 hours, (c) $850\text{ }^\circ\text{C}$ For 4 hours and (d) $950\text{ }^\circ\text{C}$ for 4 hours	27

4-5	X-Ray diffraction pattern of $\text{Sr}_{0.9}\text{Bi}_{2.1}\text{Ta}_2\text{O}_9$ synthesized at (a) 1000 °C for 2 hours, (b) 1100 °C for 4 hours and (c) 1200 °C at 4 hours	29
4-6	X-Ray diffraction patterns for $\text{Sr}_{0.8}\text{Bi}_{2.4}\text{Ta}_2\text{O}_9$ when it was heated at (a) 1000 °C for 2 hours and (b) 1100 °C for 4 hours	30
4-7	X-Ray diffraction patterns for $\text{Sr}_{0.7}\text{Bi}_{2.2}\text{Ta}_2\text{O}_9$ synthesized at (a) 1000 °C for 2 hours (b) 1100 °C for 4 hours	31
4-8	XRD patterns of $\text{SrBi}_2\text{Ta}_2\text{O}_9$ (ball milled) synthesis at (a) 850 °C for 4 hours and (b) 950 °C for 4 hours	32
4-9	Equivalent circuits of $\text{SrBi}_2\text{Ta}_2\text{O}_9$ ceramics	33
4-10	Cole-cole plot of $\text{SrBi}_2\text{Ta}_2\text{O}_9$ (solid state method) at 650 °C, 700 °C and 750 °C	35
4-11	Cole-cole plot of $\text{SrBi}_2\text{Ta}_2\text{O}_9$ (ball milling) at 650 °C, 700 °C and 750 °C	35
4-12	Cole-cole plot of $\text{Sr}_{0.9}\text{Bi}_{2.1}\text{Ta}_2\text{O}_9$ (solid state method) at 650 °C, 700 °C and 750 °C	36
4-13	Combined spectroscopic plots of $\text{SrBi}_2\text{Ta}_2\text{O}_9$ Prepared by conventional solid state method at 700 °C	37
4-14	Combined spectroscopic plot of $\text{SrBi}_2\text{Ta}_2\text{O}_9$ prepared By ball milling process at 700 °C	38
4-15	Combined spectroscopy plot for $\text{Sr}_{0.9}\text{Bi}_{2.1}\text{Ta}_2\text{O}_9$ Prepared by conventional solid state method at 700 °C	38

4-16	Variation of reactance Z'' with frequency at different Temperatures for $\text{SrBi}_2\text{Ta}_2\text{O}_9$ prepared by conventional Solid state method	39
4-17	Variation of reactance Z'' with frequency at Different temperatures for $\text{SrBi}_2\text{Ta}_2\text{O}_9$ prepared by Ball milling process	39
4-18	Variation of reactance Z'' with frequency at Different temperatures for $\text{Sr}_{0.9}\text{Bi}_{2.1}\text{Ta}_2\text{O}_9$ prepared By conventional solid state method	40
4-19	Arrhenius plot of $\text{SrBi}_2\text{Ta}_2\text{O}_9$ (solid-state method)	44
4-20	Arrhenius plot of $\text{SrBi}_2\text{Ta}_2\text{O}_9$ (ball milling)	44
4-21	Arrhenius plot of $\text{SrBi}_2\text{Ta}_2\text{O}_9$ (solid-state method)	45

LIST OF SYMBOLS / ABBREVIATIONS

ρ	resistivity, Ω
E_g	band gap energy, eV
ϵ	dielectric constant
ϵ_{\max}	maximum dielectric constant
T_c	Curie temperature, $^{\circ}\text{C}$
K	electromechanical coupling factor
Q_m	mechanical quality factor
$\text{Tan } \delta$	tangent lose
σ	conductivity
ϵ'	permittivity
E_{σ}	activation energy for conduction
Z^*	complex impedance
Z'	real impedance
Z''	imaginary impedance
ϵ_0	free space permittivity
M''	imaginary electric modulus

CHAPTER 1

INTRODUCTION

1.1 Background

Since the word “ceramics” is derived from Greek word “Keramos” which means potter’s clay or pottery, people always misunderstood that ceramics is the material that can only used to produce glassware and floor tiles objects for pottery and decorative purposes. However, today’s ceramic is also been widely used for electronic application because it has the broadest range of electrical properties of any class of material. Ceramics material that is specially formulated for specific electrical, electro-magnetic or optical properties is known as electroceramics. One of the advantages for electroceramics is its properties can be tailored to suit with the application as insulators, ferroelectric materials, highly conductive ceramics, electrode, sensor and actuator. The electroceramics development is strongly depends on the presence of ionic-covalent bonding, microstructure that comprise inorganic crystal compounds, amorphous glass in varying proportion and thermal processing conducted at elevated temperature.

Dielectric material is the main class for electroceramics. By definition, dielectric is being specified as electrical insulator that having high value in resistivity, ρ and band gap energy, E_g . Besides that, since it is polarisable, it also poses a high dielectric constant, ϵ . The dielectric constant is an important materials property where it measured the ability of an insulating material to store charge when subjected to electric field. Even though there is no charge being transferred when dielectric material is placed in an electric field, there is a redistribution of charge.

This is resulting by the formation and movement of electric dipole which are the induced dipoles and permanent dipoles. The electric dipoles had become aligned and now the material is polarized. In dielectric material, there are four possible polarization mechanisms which are electronic, ionic, dipolar and interfacial. The unique properties of dielectric material are widely applied in capacitor. For the use of capacitor, it required a high dielectric constant, high dielectric strength and low dielectric loss. Dielectric strength is the ability for a dielectric to withstand certain applied electric field strength before it break down and current flow. For the application in capacitor where the thickness of the material going to be small, high dielectric strength is an important property so that it can withstand higher electric field without degradation. Capacitor is desired to have a low dielectric loss so that the energy will not lose in the form of heat.

There are other dielectric electoceramics related properties which include ferroelectricity, pyroelectricity and piezoelectricity. The relationship for them is

- All ferroelectric are pyroelectric and piezoelectric.
- All pyroelectric are piezoelectric.
- All piezoelectric are not pyroelectric.
- All pyroelectric are not ferroelectric.

Ferroelectric material is one of the groups for dielectric material. It exhibits a dielectric dipole moment in the absence of an external electric field. The direction of the dipole moment may be switched by the application of an alternating field. This property of polarization reversal and remanence cannot be predicted by looking only at the structure of a material. Next, ferroelectrics also have an extremely large permittivity and high dielectric constant at relatively low applied frequency. Moreover, ferroelectricity is depends on temperature. Above Curie temperature, T_c ferroelectric behaviour is lost and the material becomes paraelectric. The change from the ferroelectric to the nonferroelectric state is accompanied either by a change in crystal symmetry or by an order-disorder transition. Some of the examples for ferroelectric ceramics are barium titanate ($BaTiO_3$), strontium titanate ($SrTiO_3$) and lead titanate ($PbTiO_3$). One of the most important potential applications for

ferroelectric is the incorporation as thin film into dynamic random access memories (DRAM). The majority of the memory in a computer is DRAM.

Piezoelectrics material is also another sub class for dielectric material. It exhibits a reversible property possessed by a select group of materials that does not have a center of symmetry. When a dimensional change is imposed on the dielectric, polarization occurs and a voltage or field is created. On other words it means that a voltage is produced by the means of compressive stress. This is the direct effect. On the other hand, for inverse effect, which also known as electrostriction; is occurred when an electric field is applied to dielectric and polarization cause changes in its dimension. Dielectric materials that display this reversible behaviour are called piezoelectric. The important parameter for piezoelectric is the piezoelectric constant, C/N and electrical coupling factor. Electrical coupling factor is measure of the ability of the material to convert electrical energy to mechanical energy or vice versa. The most widely used of all piezoelectric material is known as acronym PZT. Acronym PZT is the solid solution between lead zirconate ($PbZrO_3$) and lead titanate ($PbTiO_3$). PZT is widely used in making transducer for medical ultrasound imaging and are both as acoustic source and detector since it has high dielectric constant, κ and inexpensive compared to other material. Applications for piezoelectric is utilised one of the two piezoelectric effect. For direct effect of piezoelectric, it is widely used in high voltage spark generation for some gasoline ignition system, manually operated gas lighter, ignite natural gas water heaters and other gas-fired domestic application. Meanwhile, for inverse effect, piezoelectric material is to manufactured actuator. Variety types of actuator are needed for a precise mechanical control system such as in atomic force microscopy (AFM) and scanning tunnelling microscopy (STM). Moreover, piezoelectric transducers are the key components used in medical ultrasound imaging and are used both as acoustic source and detector. Microelectromechanical system (MEMS) is devices that are able to sense and respond to mechanical and electrical stimulus. Some MEMS devices that applied piezoelectric thin film are accelerometers, infrared detectors and microvalves.

Next sub class dielectric material is pyroelectric. Pyroelectric material exhibit a spontaneous polarization that is a strong function of temperature because the dipole moments vary as the crystal expands or contracts. In the seventh century, this

property was observed in the mineral tourmaline. The most common use of pyroelectricity in ceramic is LiTaO_3 . When it is subjected to a small change in temperature, the electric field developed across a pyroelectric crystal can be extremely large. For example, a crystal with a typical pyroelectric coefficient of $10^{-4} \text{Cm}^{-2}\text{K}^{-1}$ and $\epsilon = 50$ developed a field of 2000 V/cm for 1 K temperature change. Pyroelectric is widely used to detect any radiation that produces a change in the temperature of the crystal, especially for IR detection. A rise in the temperature of less than one-thousandth of a degree can be detected since pyroelectric ceramics is extremely sensitive. This property cause it widely applied in devices such as intruder alarms, thermal imaging and geographic mapping.

The material being focused in this project is strontium bismuth tantalate (SBT). The crystal structure of SBT belongs to the layered perovskite ferroelectrics where the crystal consists of stack of alternating layers of Bi_2O_2 and pseudo-perovskite SrTa_2O_7 units with double TaO_6 octahedral layers along c-axis [1]. Studies revealed that SBT structure has orthorhombic distribution with space group $A2_1am$. The layered perovskite-like ferroelectric of SBT has attraction for the development of non-volatile random access memories (NVRAMs) because of its excellent fatigue characteristic. It is believed that the present of Bi_2O_2 layers have been thought to serve as shock absorber for enduring the polarization fatigue for example the capacitors made by SBT did not show significant fatigue even after 10^{12} switching cycles. Besides that, SBT also exhibited good retention characteristic, low leakage current and low operating voltage.

In order to characterise electroceramics, it is important to know its crystal structure, microstructure, element present and properties. There are many techniques which can use to probe or distinguish between the different region of the ceramics and suitability of those characterisation techniques are depend on the type of information desired and may also be dictated by the size of sample. In this project, there are two main characterisation techniques will be carry out to characterise SBT that are XRD and Impedance Spectroscopy. Impedance Spectroscopy is a powerful technique for unravelling the complexities of electroceramics where its properties and applications is depends on the close control of structure, composition, ceramic texture and dopants distribution. Impedance spectroscopy is a general term that

subsumes the small-signal measurement of the linear electrical response of a material of interest and the subsequent analysis of the response to yield useful information about the physicochemical properties of the system. Analysis is generally carried out in the frequency domain, although measurements are sometimes made in the time domain and then Fourier transformed to the frequency domain. Impedance spectroscopy is by no means limited to the measurement and analysis of data at the impedance level but may involve any four basic immittance levels.

X-Ray diffraction (XRD) is powder diffraction for statistical determination of lattice spacing. Bragg made the first direct determination of a crystal structure using XRD, which is still generally the most accurate method for characterizing crystal symmetry. Besides that, XRD also can use to tell the phase presented but gives no direct information about their chemical constitution. When reduced to basic essentials, the X-ray diffraction requires an X-ray source, the sample under investigation and a detector to pick up the diffracted X-rays. Within this broad framework, three variables govern the different X-ray technique which is radiation, type of sample and detector.

There are lots of synthesis methods available for SBT. To synthesis SBT thin film, it can be done by different techniques such as sol-gel method, pulsed laser deposition, metallorganic chemical vapour deposition and metallorganic decomposition. For synthesization of bulk SBT ceramics powder, techniques being used are solid-state reaction, ball milling and chemical solution process for example co-precipitation and hydrothermal. For this project, ball milling and solid-state reaction will be carried out on different composition of SBT powder.

1.2 Objectives

Project objectives are

- To synthesis bismuth strontium tantalate materials
- To characterise single phase materials using X-Ray Diffusion
- To study the electrical properties using alternative impedance spectroscopy

CHAPTER 2

LITERATURE REVIEW

Recently, the ferroelectric material, strontium bismuth tantalate (SBT) had been widely investigated since it plays an important role for the application of non-volatile random access memory (NVRAM). Strontium bismuth tantalate, which is one of the bismuth layered perovskite-like structure has high potential for this application because of its high fatigue endurance and good retention. Besides that, it is also well known for its high dielectric constant, high Curie temperature, low leakage current, good ferroelectric switching characteristic and low coercive field. There are lots of methods and researches that had been done on strontium bismuth tantalate. For this chapter, the literature review is mainly focus on the different composition of strontium bismuth tantalate and strontium bismuth niobate.

2.1 SrBi₂Ta₂O₉

From the study of Li, Li, and Wang (2002), conventional solid-state reaction method has been used to prepare bulk SrBi₂Ta₂O₉ ceramics. The chemicals were mixed and ball milled for four hours using zirconia balls. The slurry is then dried at 100 °C and calcined at 1000 °C for two hours. The sintering behaviour and decomposition of bulk SrBi₂Ta₂O₉ ceramics have been investigated. It is proved that shrinkage of strontium bismuth tantalate happened when sintering temperature is increase. From the result, it shows that the pellets shrink as the temperature increases, firstly at a relatively slow rate, until about 800 °C, and then with a continuously increasing rate.

A sudden step occurs at 1350 °C. SEM fractographs of the SrBi₂Ta₂O₉ pellets shows that when temperature increases, the grain size also increases. The surface of the pellets sintered above 1100 °C was examined by XRD. Decomposition tends to start at 1200 °C and almost all the SrBi₂Ta₂O₉ disappears at 1300 °C. In order to know the effect of the length of sintering time on the decomposition of bulk SrBi₂Ta₂O₉ ceramics, the pellets were sintered at 1100 °C for different times. XRD is used to examine the surfaces of the pellets and it shows that sintering for longer than 7 hours results in decomposition of SrBi₂Ta₂O₉. In conclusion, bulk SrBi₂Ta₂O₉ ceramic can be prepared by solid-state reaction. Higher sintering temperature (more than 1200 °C) and longer sintering time (more than 7 hours) can result in decomposition of SrBi₂Ta₂O₉.

In the studies of Yang, Shi, Qin and Deng (2006), the high quality Sr₂Bi₂Ta₂O₉ ferroelectric thin film is fabricated on platinized silicon using pulsed laser deposition. It was found that the leakage current is about 3×10^{-9} A/cm² at 4V. The leakage current mechanism of the film is believed to be caused by bulk limited Poole-Frenkle emission to the increase-controlled Schottky emission with the applied field increasing and that the breakdown field of the film had a negative linear variation with the logarithm of the electrode area.

From the studies of O'Brien, Crean, Cakare and Kosec (2005) where the ferroelectric strontium bismuth tantalate thin film were deposited by thermal metalorganic chemical vapour deposition (MOCVD) onto a complex layered Pt/IrO₂/Ir/Ti(Al)N substrate. A study of ultra-violet (UV)-assisted rapid thermal processing (RTP) annealing strategies of the thin film is performed. The influence of UV-irradiated temperature and annealing atmosphere on the crystallinity of the deposited films was evaluated using both microstructure and electrical analysis technique. It was found out that the most effective crystallization of MOCVD-SBT in vacuum conditions was achieved at 350 °C, followed by a 1 hour furnace treatment at 700 °C in oxygen. Higher UV-RTP annealing temperature above 350 °C in vacuum conditions may lead to degradation of SBT perovskite film. In the case of MOCVD-SBT films processed by UV irradiation in oxygen, more effective crystallization is observed at higher temperature which is higher than 400 °C.

Annealing temperature has large effect on structural and electrical properties of $\text{Sr}_2\text{Bi}_2\text{Ta}_2\text{O}_9$. In the studies Jha, Roy, Dhar, Mannar, and Ray (2007) where the ferroelectric $\text{Sr}_2\text{Bi}_2\text{Ta}_2\text{O}_9$ thin film grown on p-type (100) Si substrate by radio frequency sputtering technique, shows the crystallinity is largely depend on the annealing temperature. The perovskite phase of SBT diffraction peak became predominant at higher annealing temperature. Besides that, it is also revealed that there is increase of cluster size with the increase of substrate temperature. It is reported that surface roughness of the film had increase sharply with increase annealing temperature from 700 °C to 800 °C which might due to the poor interface between SBT thin film and silicon substrate at higher annealing temperature. Thus, it would be better if the annealing temperature is lower than 800 °C. This statement is again being proved by Gao, Erjia, Zhibin, Jianqing and Aiping (2003) where $\text{Sr}_2\text{Bi}_2\text{Ta}_2\text{O}_9$ were fabricated on Pt/Ti/SiO₂/Si(100) substrate by pulsed laser excimer deposition (PLD). It is reported that deposition of SBT on Pt/Ti/SiO₂/Si(100) substrate at 400 °C followed by annealing process at 700 °C is believed to be an optimized process for the film.

In comparison, from the studies of Zanetti et al. (2004), it stated that with the use of commercial technique, in order to obtain well crystallized of SBT film with ferroelectric properties, relatively high temperature is required (approx. 800 °C) and the film must keep at this high temperature at least 1 hour. The long thermal treatment may lead to serious damage to the stack, leading to interdiffusion between the element of the film and substrate which resulting loss of films' stoichiometry. Thus, it is important to use low processing temperature so that the properties of ferroelectric systems can be optimized. In this report, $\text{SrBi}_2\text{Ta}_2\text{O}_9$ thin film which produced by polymeric precursor method were crystallized at low temperature using a domestic microwave oven. A SiC susceptor was used to absorb the microwave energy and rapidly transfer heat to the film. Low microwave power and short time had been used. No post annealing process was needed during the process. As the result, the film that successfully obtained at 600 °C for 10 mins is crack-free, well-adhered and fully crystallized. This result also represents a significant improves in time, which at least 3 times less when using the microwave oven. The microstructure displayed a polycrystalline nature with an elongate grain size compared to the films

obtained by conventional treatment. The dielectric constant values are 240, 159 and 67 for the films treated at 600 °C, 650 °C and 700 °C which show lower treatment temperature leads to high dielectric constant. Electrical measurement revealed that the increase of temperature of the treatment to 700 °C causes a complete loss of ferroelectricity due to the effect of the microwave energy and resulting degradation of the film/electrode interface. This problem was being improved by placing a 4 mm thick ceramic wool between the SiC susceptor and the substrate.

Many researches had been done on mechanochemical activation in a high energy ball mill using powder mixture. This technique is basically used to synthesis metallic alloys and intermetallic compounds that either have very complex compositions or have melting temperatures very high to prepare by conventional melting or alloying. In the studies of Sritharan, Boey and Srinivas (2007), investigation had been done on solid state synthesis of three complex ceramics which are nickel ferrite, manganese ferrite and strontium bismuth tantalate by mechanochemical activation in a high energy ball mill. However, only the result of strontium bismuth tantalate is being concerned in this project. By using XRD, it had found out that a stoichiometric powder mixture of SrCO_3 , Bi_2O_3 , and Ta_2O_5 corresponding SBT did not show any synthesis of SBT during the milling process up to 50 hours. Milling appears leads to the dissolution in Bi_2O_3 of other oxides. It was shown that mechanochemical activation prior to reaction synthesis at elevated temperature is generally beneficial to reduce the necessary synthesis temperature. It is reported that subsequent heating to 650 °C resulted in complete synthesis of SBT which in comparison to those unmilled powder of the same composition required heating to above 1000 °C for the synthesis of SBT. These results are been supported by Chew, Srinivas, Sritharan and Boey (2005), since same results had been obtained. In the report, it had shown that the average powder particle size is reduced to about 480 nm from initial size of 900 nm. It had found that after milling for 25 hours, there is a sharp decrease of average particle size. Besides that, after 40 hours of milling, the particles become almost spherical and uniform in size in contrast to a large size distribution evident at shorter milling time. From the experiment, the author conclude that the reason for activating the reaction at lower temperature is the metastability of the as-milled powder.

Usually, nanocrystalline of strontium bismuth tantalate was prepared based on solution based chemical route since it not only reduced the processing temperature for material synthesis but they also efficiently control the morphology, chemical homogeneity and stoichiometry of the material through molecular level mixing of the starting compound in the solution. In the study of Asit, Abhijit, Amita, and Panchanan (2004), nanocrystalline $ABi_2Ta_2O_9$ ($A = Sr^{2+}/ Ba^{2+}/ Ca^{2+}$ ion) powders is prepared through decomposition of mixed metal complexes based aqueous precursor solution. However, since the project is mainly focus for strontium bismuth tantalate, nanocrystalline of $BaBi_2Ta_2O_9$ and $CaBi_2Ta_2O_9$ will not be discussed in this chapter. The synthesis of the pure crystalline of $SrBi_2Ta_2O_9$ through evaporation of a mixture of tantalum tartarate and other metal ion complex solutions followed by calcinations at comparatively low temperature which is between 700-750 °C had been developed. The use of soluble tantalum-tartarate as tantalum source is found to be an efficient alternative for the preparation of any tantalum based mixed oxides since it is cheap, does not involve the problem of moisture sensitivity and hydrolysis. Using this method, under sintering process at 700 to 750 °C for two hours yields the single phase $SrBi_2Ta_2O_9$ powder with crystallite size around 12 to 17 nm. Due to the low sintering temperature (700 to 750 °C) and phase formation, the problem of bismuth evaporation is avoided. The dielectric constant values for sintered pellets of Sr have found to be 1387 at the respective Curie temperature of 279 °C. On the other hand, by using tartarate-triethanolamine (TEA) to prepare the SBT nanocrystalline powder as stated in the same authors' report of Asit, Abhijit and Panchanan (2003), similar amount of dielectric constant is achieved at the Curie temperature but the smallest particle size obtained is 15 nm. Bismuth evaporation also been successfully prevented through efficient low temperature sintering.

2.2 $\text{Sr}_{0.8}\text{Bi}_{2.6}\text{Ta}_2\text{O}_9$

From the studies of Huang, Chou, Lian, and Tseng, (2004), fluorite-like $\text{Sr}_{0.8}\text{Bi}_{2.6}\text{Ta}_2\text{O}_9$ (SBT) had been investigated in term for its electrical and dielectric behaviour. The fluorite-like $\text{Sr}_{0.8}\text{Bi}_{2.6}\text{Ta}_2\text{O}_9$ was spin-coated on Ir (50nm)/ SiO_2 (100nm)/ p-type (100) Si substrate using the metal-organic decomposition (MOD) technique. The fluorite-like $\text{Sr}_{0.8}\text{Bi}_{2.6}\text{Ta}_2\text{O}_9$ films deposited using this technique and heated at 450 °C or longest duration of 60 minutes had a linear dielectric or paraelectric phase with dielectric constant of 100. This was because SBT films of cubic fluorite phase has linear dielectric property and does not have any ferroelectric characteristic. The 450 °C annealed films had the low leakage current density of about 4×10^{-8} A/cm² at 200 kV/cm. The dependence of cumulative failure on dielectric breakdown field and time-dependent dielectric for these paraelectric SBT film indicated that the longer annealing time, the better the breakdown field owing to the lower leakage current density and better crystallinity with larger dielectric constant. In comparison, ferroelectric thin film of bismuth layer structured compounds; $\text{Sr}_{0.8}\text{Bi}_{2.6}\text{Ta}_2\text{O}_9$ stated in the studies of Chou, Chen, and Tseng (2003) had used the same technique as in report of Huang et al.. The leakage current density and dielectric constant of the SBT films were strongly dependent on the annealing temperature. Leakage current density is decreasing with annealing temperature. The thin film annealed at 450 °C has a low leakage current of 10^{-9} A/cm² at an applied field of 100 kV/ cm. On the other hand, the dielectric constant is increasing with temperature. The lowest leakage current density and change on dielectric constant with annealing temperature is different between ferroelectric SBT and fluorite-like paraelectric SBT which had a linear dielectric. Besides that, increase in annealing temperature also results an increase in grain size, mean surface roughness and inter diffusion through interfacial layers. On the other hand, the composition analysis of SBT thin films also indicated a loss at higher annealing temperature due to the bismuth evaporation and diffusion into the bottom electrode.

2.3 Non-stoichiometric $\text{Sr}_{1-x}\text{Bi}_{2+2x/3}\text{Ta}_2\text{O}_9$ ceramics

In the study of Rajni, Vinay, Abhai and Sreenivas (2004), ferroelectric and piezoelectric properties of non-stoichiometric strontium bismuth tantalate (SBT) [$\text{Sr}_{1-x}\text{Bi}_{2+2x/3}\text{Ta}_2\text{O}_9$] ceramics with $x= 0.0, 0.15, 0.30$ and 0.45 prepared from sol-gel derived powder is compared. It had found that a single homogenous phase is produced up to $x= 0.15$ when it is sintering at $1000\text{ }^\circ\text{C}$. An undesired BiTaO_4 phase tends to be detected with $x > 0.15$ and a higher sintering temperature ($1100\text{ }^\circ\text{C}$) prevent the formation of this phase. The ferroelectric to paraelectric phase transition temperature (T_c) increase linearly from 325 to $455\text{ }^\circ\text{C}$ up to $x= 0.30$ and with $x > 0.30$, it tends to deviate from the linear behaviour. At $x= 0.30$ has the highest transition temperature and thus the peak of dielectric constant (ϵ'_{max}) is highest while on the other hand, at $x=0.45$, a broad and a weak transition is observed and ϵ'_{max} is significant reduced which is mainly caused by the present of mixed phase. In the report, it shows that the electrical properties tend to degrade for $x > 0.30$ are attributed to the presence of undesired BaTiO_4 phase which is difficult to identify in the analysis due to the close proximity of the peak position of BaTiO_4 and the SBT phase. The surface morphology of the four compositions of SBT ceramics are obtained on the fracture SBT surface using SEM. Measurement up to $x=0.30$ exhibited a uniform distribution of densely packed grains, and the average grain size is increase with x (0 to 0.30). The sintered sample with $x=0.45$ had shown that the grains and grain boundaries were found to be unclear. A lot of porosity was observed indicating a decrease in density.

The effect of non-stoichiometric on the ferroelectricity and piezoelectricity of strontium bismuth tantalate has been studied in Chie, Rintaro, Hiraoki, Soichiro and Tadashi (2005) using ordinarily fired ceramics. $\text{Sr}_{1-x}\text{Bi}_{2+2x/3}\text{Ta}_2\text{O}_9$ ($x= 0.0-0.30$) ceramics were prepared by conventional ceramics technique and sintered at $1200\text{ }^\circ\text{C}$. It had reported that the maximum electromechanical coupling factors (k_p and k_{33}) and mechanical quality factor Q_m were obtained for an SBT at around $x=0.2$. The reduction of the piezoelectric properties $x > 0.2$ was found. This phenomenon is due to the decrease in the electric resistivity of SBT ceramics. In conclusion, both the

ferroelectric and piezoelectric properties of SBT ceramics are enhanced by the Bi substitution.

2.4 Strontium Bismuth Niobate (SBN)

There are similarities between strontium bismuth tantalate and strontium bismuth niobate. Both of them also are Bi-layered perovskite that is belong to Aurivillius family, thus have high fatigue resistance which resulting its suitability to use in non-volatile random access memory (NVRAM) application. In this section, some synthesis process and properties of strontium bismuth niobate will be discussed.

Synthesis and characterisation of ferroelectric $\text{SrBi}_2\text{Nb}_2\text{O}_9$ can be done using an aqueous acetate-citrate precursor gel as stated in Nelis et al. (2005) which offers a low cost and environmental friendly alternative to the conventional sol-gel techniques since the available salt is easily dissolved in water. From the TEM experiments of free standing thin film showed that the precursor homogeneity was maintained throughout the entire thermo-oxidative decomposition of the sol gel. The phase formation of SBN also is studied using high temperature X-ray diffraction (HT-XRD). The results shows that at about 425 °C, the intermediate fluorite phase tends to crystallized out of the amorphous precursor, immediately after the release of the metal ions from the organic network. The onset temperature for transformation into the ferroelectric perovskite phase is dependent upon the Bi^{3+} -content where the Bi^{3+} -excess sample shows a higher perovskite to fluorite ratio at 625 °C compared to stoichiometric sample. An interesting observation is that the excess Bi^{3+} does not lead to the formation of the Bi_2O_3 secondary phase which indicated that the processing temperature of SBN can be lowered by changing the metal ion ratio of the precursor solution. In comparison, synthesis the nano-sized layered ferroelectric ceramics layered $\text{SrBi}_2\text{Nb}_2\text{O}_9$ through the pyrolysis of coordination compounds of metal ions as stated in Dhak, Biawas and Pramanik (2006) had found that there is no intermediate phase presented during the heat treatment at and above 600 °C compared where there is presence of intermediate fluorite phase at 425 °C. XRD

showed that after calcining at 600 °C, a single phase with the layered perovskite structure of SBN was formed. This aqueous synthesis of the perovskite phase of the ferroelectric perovskites $\text{SrBi}_2\text{Nb}_2\text{O}_9$ at reduced temperature is also proved to be environmental friendly as the aqueous acetate-citrate precursor gel technique since the use of Sr-EDTA, Bi-EDTA, and Nb-tartarate have been very effective. The crystallite size and the effective strains were found to be 38.8 nm and 0.01475, respectively while the particle size lay between 25 and 36 nm. Besides that, the average grain size after sintering at 900 °C for 4 hours was 0.67 μm . Dielectric properties obtained by this synthesis method is significant high. The study revealed that dielectric constant increased with temperature and reach a maximum (ϵ_{max}) at the Curie temperature (T_c) at 450 °C. At frequency 1 kHz, the dielectric constant is sharply increased with temperature even after the Curie temperature and the value of dielectric constant at 450 °C is 1970. As studied in Zanetti et al. (2003), new method had been developed for the synthesis of $\text{SrBi}_2\text{Nb}_2\text{O}_9$ which is known as combustion synthesis. Strontium nitrate, niobium ammonia oxalate and bismuth oxide were used as oxidant and urea as fuel. The influence of the fuel proportion on powders characteristics was evaluated by the addition of different fuel amount. In the report, the as synthesized stoichiometric powder presented a mean particle size and a crystallite size of 62.4 and 15.7 nm, respectively. It had found out that an increase in the fuel proportion leads to increase in the mean particle size due to the higher temperature reached during the reaction. Consequently, it increases the degree of agglomeration in these powders. The pellet prepared with the stoichiometric powder presents a ferroelectric-paraelectric transition at Curie temperature.

Preparation of single crystalline $\text{Sr}_{0.5}\text{Ba}_{0.5}\text{Nb}_2\text{O}_6$ particles was been done in the studies of Chen, Shoichi, Cihangir and Koji (2006) by self assemble process. Single crystal and agglomerate-free SBN50 particles were successfully prepared by molten state synthesis, while the solid state reaction method resulted in severe agglomeration of particle. In molten state synthesis, pure SBN50 phase may be obtained at 950 °C and 1:1 weight ratio of oxides and salt. When temperature and salt amount increase, $\text{SrBi}_2\text{Nb}_2\text{O}_9$ phase starts to appear. The synthesis particles are faceted, sub-micrometer and have an anisotropic morphology along c-axis. The aspect ratio of SBN particles reduced with increase in the amount of salt, while the

synthesis temperature does not shows much influence on the particle morphology between 950 and 1000 °C. Incorporation of Na⁺ and K⁺ ions are found in SBN50 lattice. Molten salt synthesis method for synthesized SBN50 particles is found to be suitable for the preparation of grain-oriented ceramics by self-assemble process.

CHAPTER 3

METHODOLOGY

3.1 Introduction

There are many techniques that can be used to synthesis strontium bismuth tantalate, such as sol-gel method, thermal metalorganic chemical vapour deposition and aqueous acetate-citrate precursor gel. However, in this project, strontium bismuth tantalate is chose to be sintered by solid state reaction of component oxide mixtures at high temperature and by high energy ball mill. Solid state reaction is the method which used to mix the powder reactants together and synthesis at high temperature. After that, pressure is applied to press them into pellets. After that, the pellets are heated in furnace for a period of time. This method is considered to be very effective and easy to perform and thus, it is been widely used for the preparation of high T_c superconductors. In contrast, the disadvantage of using solid state reaction method is it required high reaction temperature which in turn coarsening the grains of the material and affects the sintering properties. Next, it provides a limit in the degree of chemical homogeneity. Although the reactants may be well mixed at the level of individual particles, but on the atomic level, they are inhomogeneous. As the result, solid state reaction method is intrinsically slow. Therefore, in order to bring atoms of the different elements together, it required an enormous amount of mixing atoms or ions. Besides that, correct ratio of the strontium bismuth tantalate is necessary so that desired product can be obtained. There is a way to accelerate the reaction which is frequently grinding the partially reacted mixture during the process. A small amount of liquid transporting agent also can effective in giving enhanced reaction rate.

There is an alternative to overcome the high reaction temperature of solid state reaction method by using ball milling process since it had been proved to reduce the synthesis temperature, thus eliminate the effects of grains coarsening and affect sintering properties. The main advantage of the process is that it provided a situation of intense energy in localized parts of the load where solid state diffusion and dissolution are forced on, even though the resulting material may be thermodynamically unstable. Frequently, metastable structures, solid solutions and phases are formed.

3.2 Sample Preparation

Strontium bismuth tantalate, $\text{Sr}_{1-x}\text{Bi}_{2+x/3}\text{Ta}_2\text{O}_9$ ($x = 0.0, 0.1, 0.2, 0.3$) was synthesized by conventional solid state sintering while solid state sintering with ball milling was performed only on $\text{Sr}_{1-x}\text{Bi}_{2+x/3}\text{Ta}_2\text{O}_9$ ($x = 0.0$ and 0.3). For both solid state sintering methods, the sample preparation were started with drying the high purity oxide, SrCO_3 , Bi_2O_3 and Ta_2O_5 in the furnace to remove any moisture prior to weighing. SrCO_3 also needs to be converted into SrO . Bi_2O_3 was heated at $300\text{ }^\circ\text{C}$ while Ta_2O_5 at $600\text{ }^\circ\text{C}$ in the furnace, each for half an hour. For SrCO_3 , to transform SrCO_3 to SrO , it required to heat treated in furnace at $1100\text{ }^\circ\text{C}$ for 1 hour.

For conventional solid state reaction, stoichiometric quantities of the oxides were weighted at 1.5 g and mixed with sufficient amount of acetone to ensure the homogeneity of the mixture. It was then grounded in an agate mortar. The mixture was dried and fired in alumina boat at $1100\text{ }^\circ\text{C}$ for 4 hours in a Carbolite furnace with intermittent regrinding to increase the contact area of the reactants. On the other hand, for solid state reaction with ball milling process, the stoichiometric mixture of oxide powder was milled for 4 hours in tempered steel vials. Milling of the mixture had to be stopped and shook the bottle from time to time in order to minimise the temperature rise due to friction. The mixture are dried and fired at $950\text{ }^\circ\text{C}$ for 4 hours. The samples were finally pressed into block and ready for further analysis.

3.3 Characterisation

3.3.1 XRD

In order to determine the crystalline phase identity and purity of the samples, X-ray diffraction technique (XRD) is used. The XRD data obtained were used for refinement using Checkcell programme with angular tolerance of $0.1^\circ 2\theta$. The cell parameters of the samples can then be calculated. The pure (single phase) sample will then be used for determination of electrical properties using impedance analyzer.

3.3.2 Impedance Studies

Pellets with 10 mm diameter and 1.5 mm thick were cold pressed with pressure of about 50 kg/cm^3 using a hydraulic press and held for 30 seconds. The pellets were then sintered at 1200°C for 2 hours to increase their mechanical strength and reduce the intergranular resistance in the pellets. The ceramics were then being smeared and hardened by gold paste onto their parallel faces. The pellets with gold electrode attachment were placed on a conductivity jig and inserted horizontally into the tube furnace. The electrical properties were studied using a Solartron Schlumberger SI 1260 impedance/gain analyser with frequency range of 5 Hz to 13 MHz. The measurements were made from room temperature (28°C) to 800°C by increment step of 100°C from room temperature to 400°C while from 400°C to 800°C , the increment step is 50°C with 30 minutes of stabilization time.

3.4 Flow chart

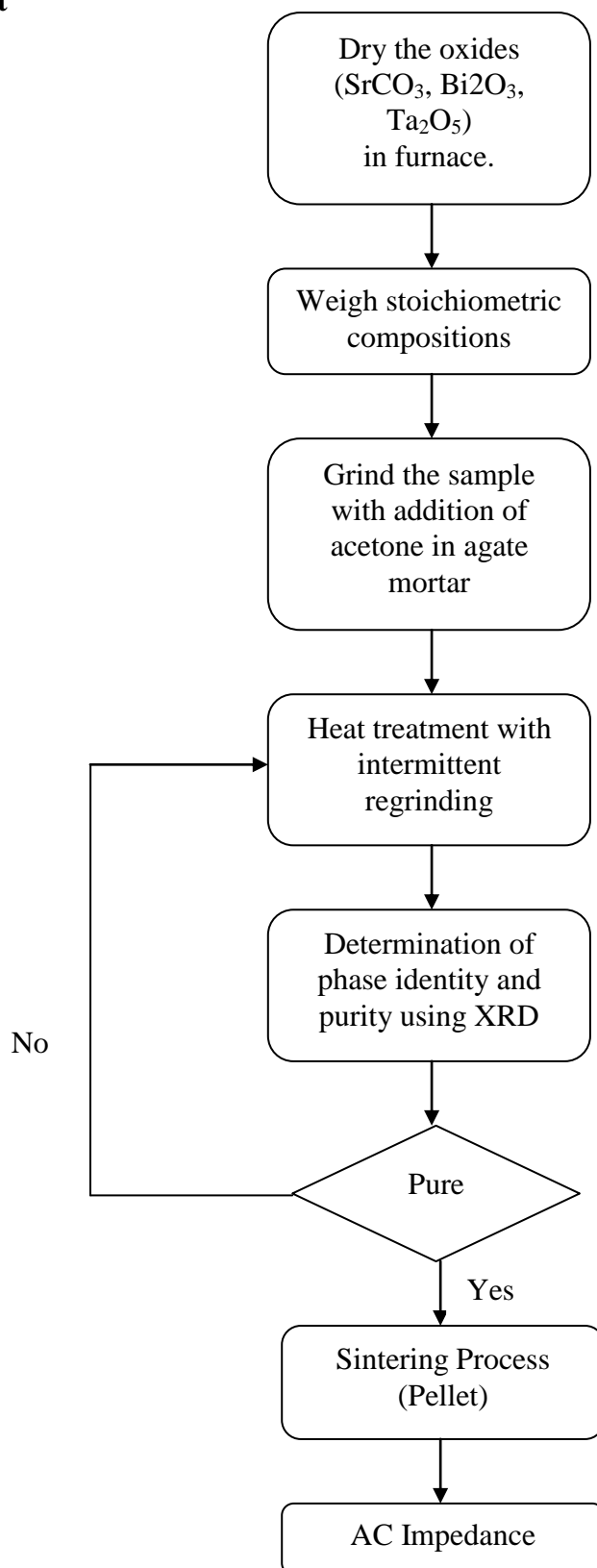


Figure 3.1 Flow chart for sample preparation with conventional solid state sintering method and characterisation

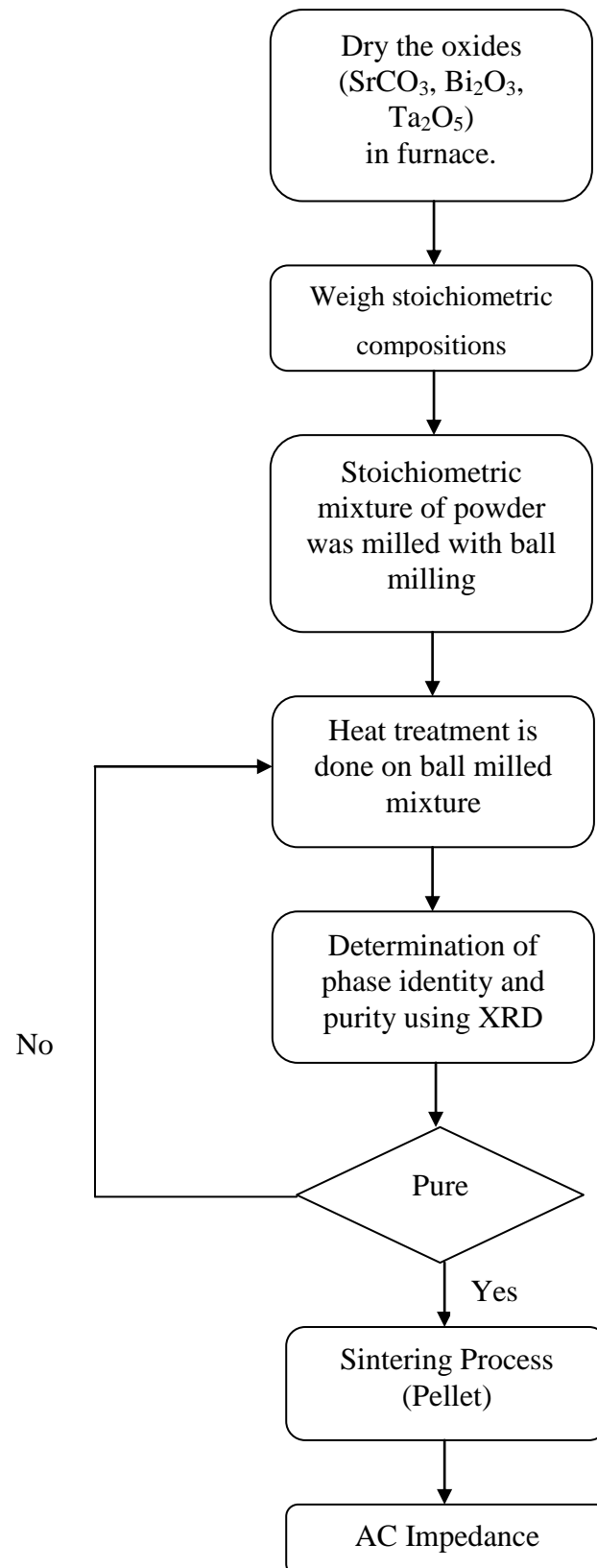


Figure 3.2 Flow chart for sample preparation using solid state sintering method with ball milling and characterisation

3.5 Gantt Chart

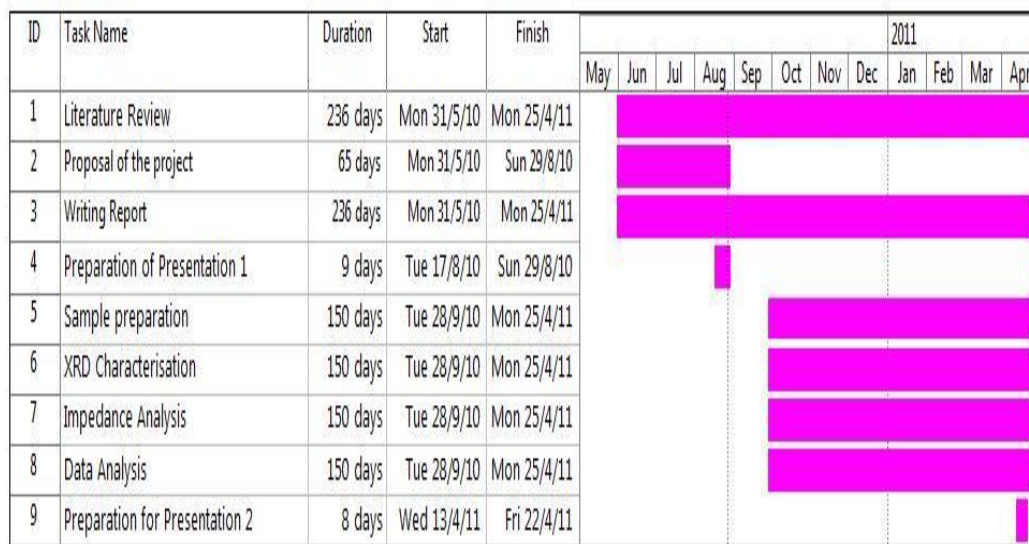


Figure 3.3 Gantt chart for the project

CHAPTER 4

RESULTS AND DISCUSSIONS

4.1 XRD Analysis

Figure 4.1 shows the XRD patterns of $\text{Sr}_{1-x}\text{Bi}_{2+2x/3}\text{Ta}_2\text{O}_9$ ($x=0, 0.1, 0.2, 0.3$) prepared by conventional solid state method. Few impurity phases correspond to BiTaO_4 , Bi_3TaO_7 and certain unknown phases are observed in the sample of $x=0.2$ ($\text{Sr}_{0.8}\text{Bi}_{2.4}\text{Ta}_2\text{O}_9$) and $x=0.3$ ($\text{Sr}_{0.7}\text{Bi}_{2.2}\text{Ta}_2\text{O}_9$), synthesized at $1100\text{ }^\circ\text{C}$. This is consistent with the result in literature, in which the single homogeneous material can only be obtained when $x < 0.15$, at the synthesized temperature of $1100\text{ }^\circ\text{C}$ (Rajni, Vinay, Abhai and Sreenivas, 2004). However, in this study, a tiny peak of BiTaO_4 is observed at $\sim 30\text{ }2\theta^\circ$ for composition of $x=0$ ($\text{SrBi}_2\text{Ta}_2\text{O}_9$) and $x=0.1$ ($\text{Sr}_{0.9}\text{Bi}_{2.2}\text{Ta}_2\text{O}_9$). This tiny peak can be negligible since it is relatively very small in intensity and those samples are deemed to be phase pure. Increasing of the synthesis temperature to $1200\text{ }^\circ\text{C}$ would result in partially melting of the sample.

Figure 4.2 shows the XRD patterns of $\text{Sr}_{1-x}\text{Bi}_{2+2x/3}\text{Ta}_2\text{O}_9$ ($x=0$ and 0.3) prepared by ball milling process. According to literature, 50 hours of ball milling followed by subsequent heating to $650\text{ }^\circ\text{C}$ lead to complete synthesis of the single phase of strontium bismuth tantalate material (Sritharan, Boey and Srinivas, 2007). However, in this project, some impurity phases are observed in $\text{SrBi}_2\text{Ta}_2\text{O}_9$ and $\text{Sr}_{0.7}\text{Bi}_{2.2}\text{Ta}_2\text{O}_9$ samples even with higher synthesized temperature, $950\text{ }^\circ\text{C}$. This might be due to the limited ball milling time used in the project, causing the samples not yet achieved equilibrium.

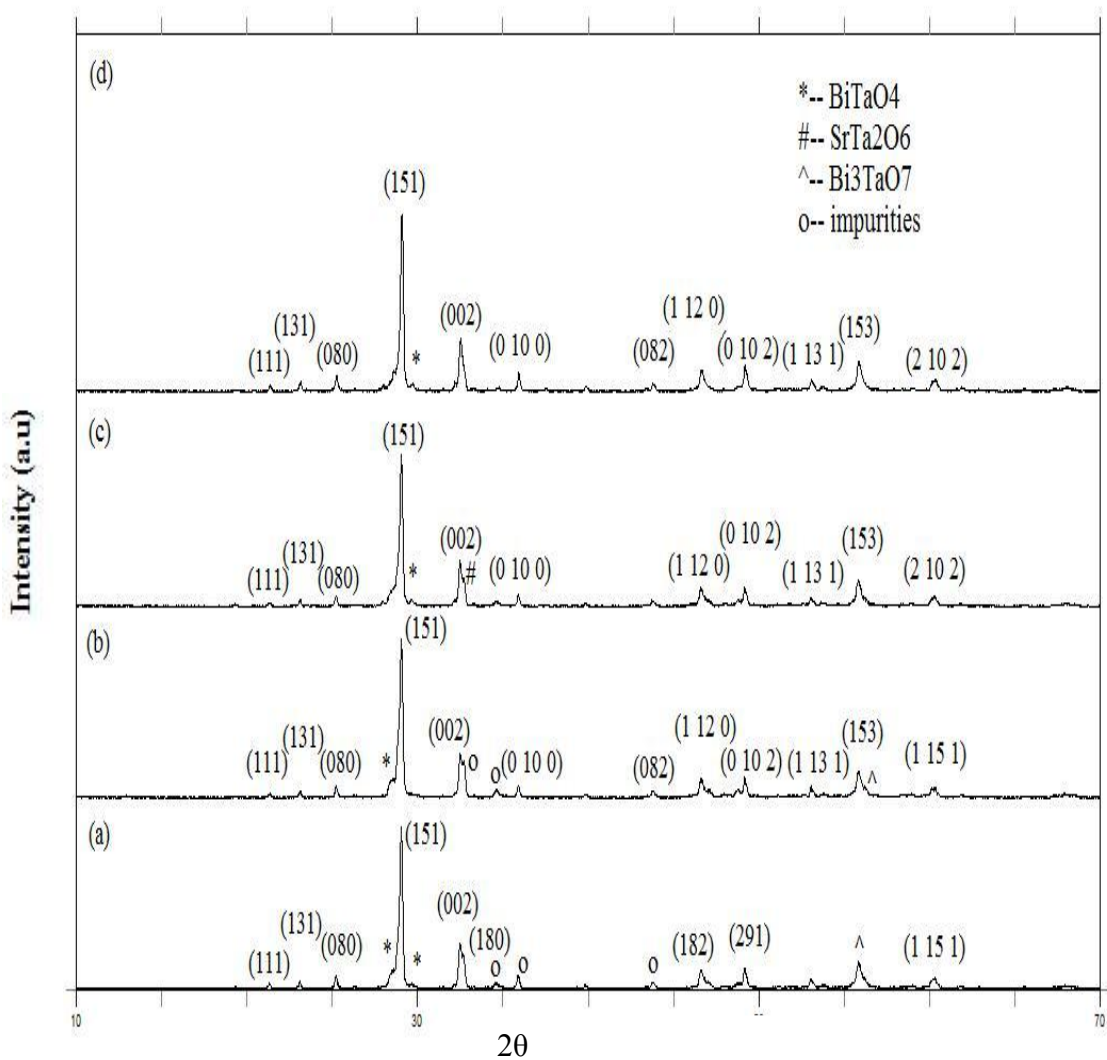


Figure 4.1 X-Ray diffraction patterns of $\text{Sr}_{1-x}\text{Bi}_{2+2x/3}\text{Ta}_2\text{O}_9$ ceramics (a) $x=0.3$ (b) $x=0.2$ (c) $x=0.1$ and (d) $x=0$ prepared by conventional solid state method.

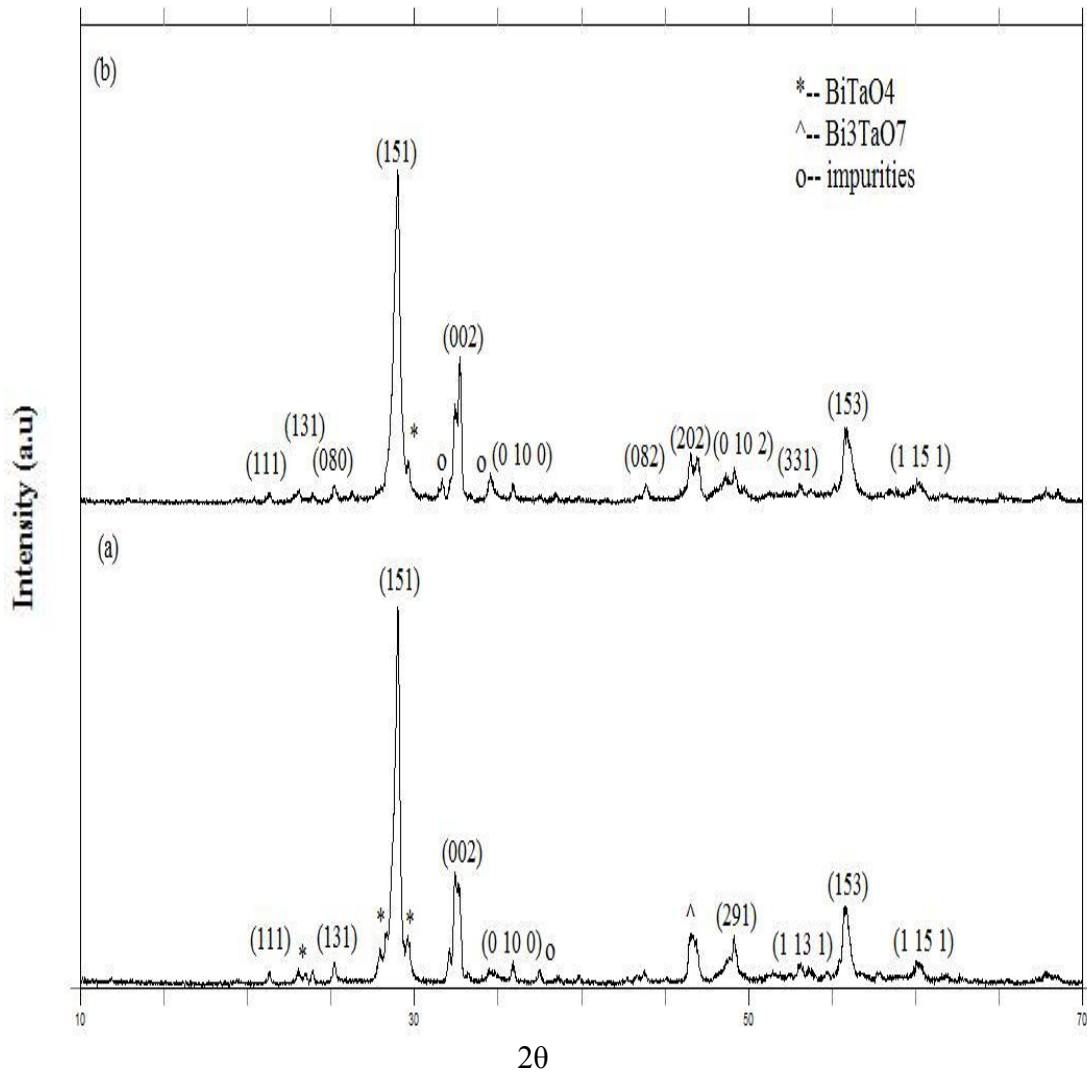


Figure 4.2 X-Ray diffraction patterns of $\text{Sr}_{1-x}\text{Bi}_{2+2x/3}\text{Ta}_2\text{O}_9$ ceramics (a) $x= 0.3$ and (b) $x= 0$ prepared by ball milling process.

4.1.1 Phase Formation Study of $\text{SrBi}_2\text{Ta}_2\text{O}_9$ (Solid-State Method)

Figure 4.3 shows the XRD patterns of $\text{SrBi}_2\text{Ta}_2\text{O}_9$ synthesized at a) 1000 °C for 2 hours b) 1000 °C for 4 hours and c) 1100 °C for 4 hours respectively. Many impurity peaks are observed for sample synthesized at 1000 °C for 2 hours. As synthesis time increased, some of the phases diminished mainly because the sample was more time to react and thus enhance the crystallinity of this compound. Finally, phase pure $\text{SrBi}_2\text{Ta}_2\text{O}_9$ are obtained at 1100 °C with heating temperature of 4 hours. The refined lattice parameters are $a = 5.5421 \text{ \AA}$, $b = 24.9833 \text{ \AA}$ and $c = 5.5007 \text{ \AA}$, $\alpha = \beta = \gamma = 90^\circ$.

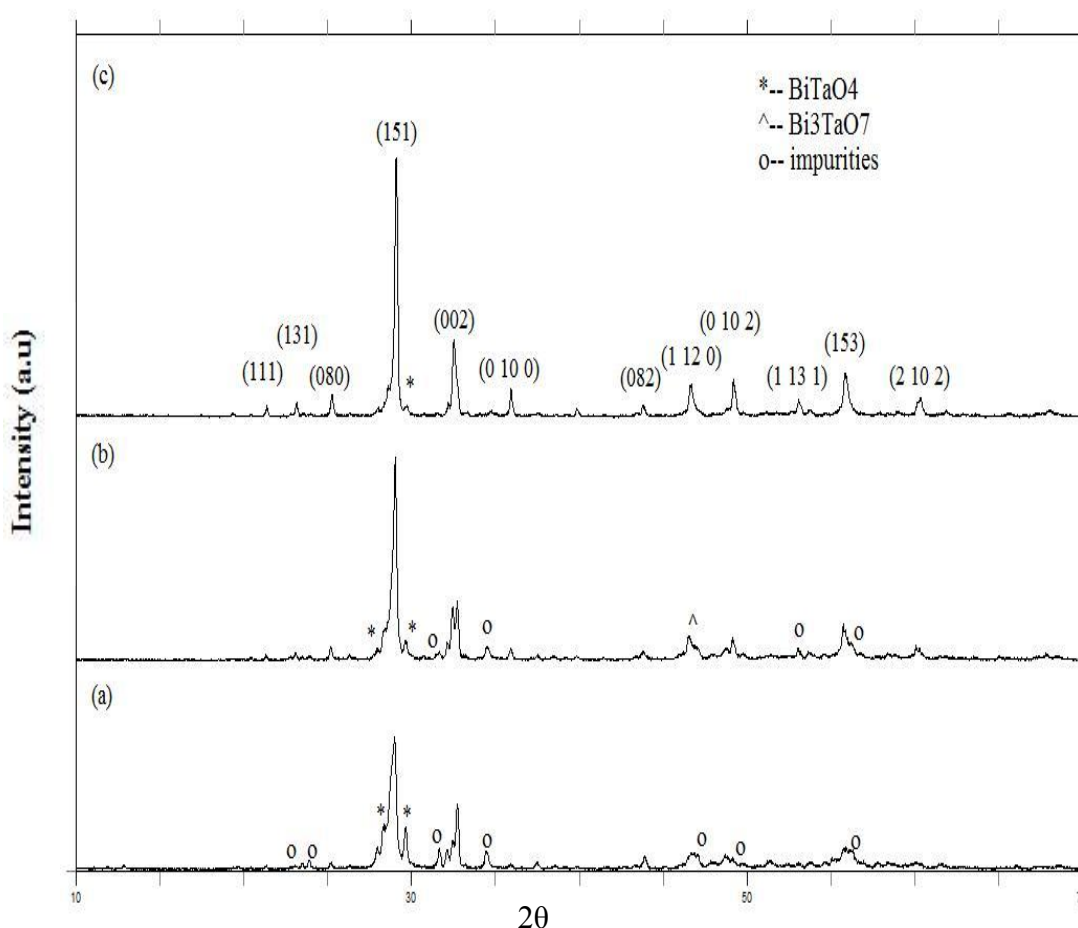


Figure 4.3 X-ray diffraction patterns of $\text{SrBi}_2\text{Ta}_2\text{O}_9$ (solid-state) synthesized at a) 1000 °C for 2 hours b) 1000 °C for 4 hours and c) 1100 °C for 4 hours.

4.1.2 Phase Formation Study of $\text{SrBi}_2\text{Ta}_2\text{O}_9$ (Ball Milling)

Figure 4.4 shows the XRD patterns of ball milled $\text{SrBi}_2\text{Ta}_2\text{O}_9$ sample synthesized at (a) 650 °C for 2 hours, (b) 650 °C for 4 hours, (c) 850 °C for 4 hours and (d) 950 °C for 4 hours, respectively. $\text{SrBi}_2\text{Ta}_2\text{O}_9$ heated for 2 hours at 650 °C, shows a large number of impurities and splitting of peak ~ 28 2 θ° . With the increase of heating duration to 4 hours, the number of impurity peaks is reduced, splitting of peak at ~ 28 2 θ° still visible. This indicates that the reaction is incomplete even with the increase in heating time, thus a higher heating temperature is needed. With increased synthesis temperature to 850 °C, certain impurity phases are diminished and splitting of peak is not visible. Further heat treatment at 950 °C has greatly reduced the impurity peaks and a single phase material is nearly obtained. The refined lattice parameters are $a = 5.5699$ Å, $b = 25.0823$ Å and $c = 5.4935$, $\alpha = \beta = \gamma = 90^\circ$, respectively.

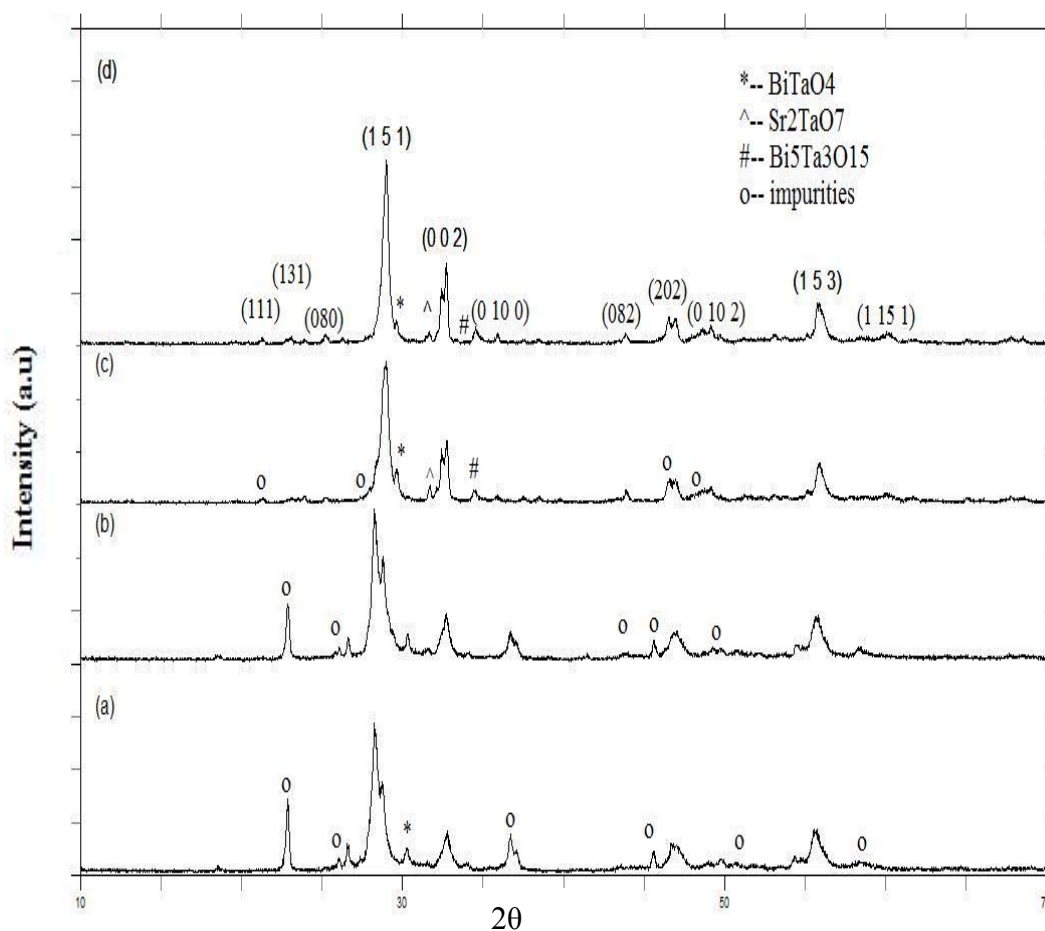


Figure 4.4 XRD patterns of $\text{SrBi}_2\text{Ta}_2\text{O}_9$ (ball milled) synthesis at (a) 650 °C for 2 hours, (b) 650 °C for 4 hours, (c) 850 °C for 4 hours and (d) 950 °C for 4 hours.

4.1.3 Phase Formation Study of $\text{Sr}_{0.9}\text{Bi}_{2.1}\text{Ta}_2\text{O}_9$ (Solid-State Method)

Figure 4.5 shows the XRD patterns of $\text{Sr}_{0.9}\text{Bi}_{2.1}\text{Ta}_2\text{O}_9$ synthesized at (a) 1000 °C for 2 hours, (b) 1100 °C for 4 hours and (c) 1200 °C at 4 hours respectively. Sample heated at 1000 °C for 2 hours, unable to yield single phase, with the presence of many impurity peaks. Hence, higher synthesis temperature and longer heating duration needed for the sample to complete reacted. Further heat treatment for 4 hours at 1100 °C enhances the crystallinity of the compound, proven by the reduction of impurity peaks (Figure 4.5 (b)). In the study of Lu and Lee (1998), SrTa_2O_6 tend to coexist with $\text{SrBi}_2\text{Ta}_2\text{O}_9$ at 1250 °C and further heat treatment at 1300 °C led to decomposition of $\text{SrBi}_2\text{Ta}_2\text{O}_9$. At 1300 °C, the vapour pressure of Bi_2O_3 was quite high and would be evaporated out. This is consistent with the result obtained in this study. However, in the current study, the reactions happened at a lower temperature; exists SrTa_2O_6 at 1100 °C. Decomposition of $\text{SrBi}_2\text{Ta}_2\text{O}_9$ and the evaporation of Bi_2O_3 start at 1200 °C. In this study, synthesis condition is chosen as 1100 °C, 4 hours because sample will be partially melted at 1200 °C. The refined lattice parameters are $a= 5.5046 \text{ \AA}$, $b= 25.0056 \text{ \AA}$ and $c= 5.546 \text{ \AA}$, $\alpha= \beta= \gamma = 90^\circ$, respectively.

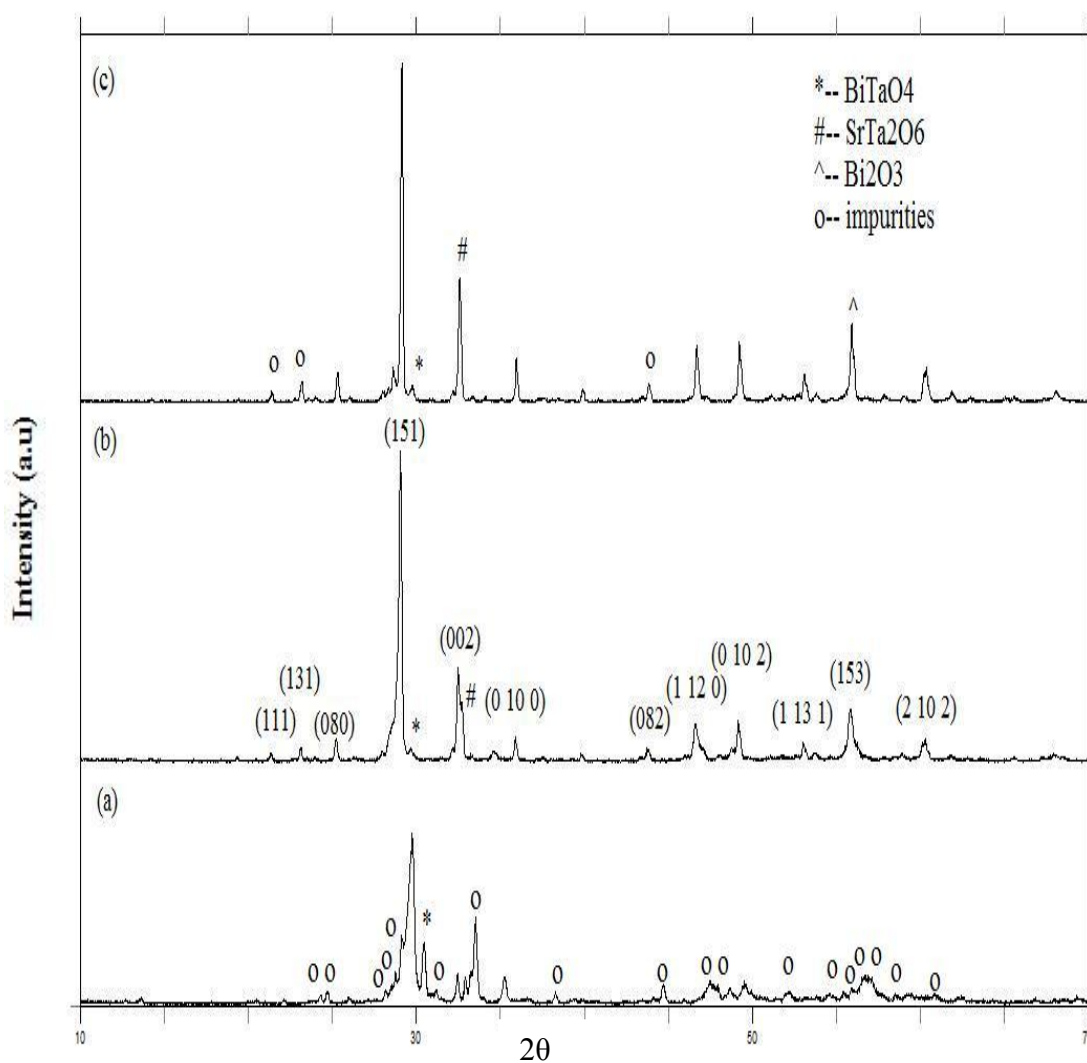


Figure 4.5 X-Ray diffraction pattern of $\text{Sr}_{0.9}\text{Bi}_{2.1}\text{Ta}_2\text{O}_9$ synthesized at (a) 1000 °C for 2 hours, (b) 1100 °C for 4 hours and (c) 1200 °C at 4 hours.

4.1.4 Phase Formation Study of $\text{Sr}_{0.8}\text{Bi}_{2.4}\text{Ta}_2\text{O}_9$ (Solid-State Method)

Figure 4.6 shows the XRD patterns for $\text{Sr}_{0.8}\text{Bi}_{2.4}\text{Ta}_2\text{O}_9$ synthesized at (a) 1000 °C for 2 hours and (b) 1100 °C for 4 hours. Many impurity phases such as BiTaO_4 , Bi_3TaO_7 and unidentified compound are observed in Figure 4.6 (a). Further heat treatment at 1100 °C for 4 hours reduces the impurity peaks and yields a nearly pure sample. The synthesis condition is set as 1100 °C for 4 hours because higher temperature will lead to partial melt of the sample. The refined lattice parameters are $a = 5.5423 \text{ \AA}$, $b = 24.9915 \text{ \AA}$ and $c = 5.5069 \text{ \AA}$, $\alpha = \beta = \gamma = 90^\circ$, respectively.

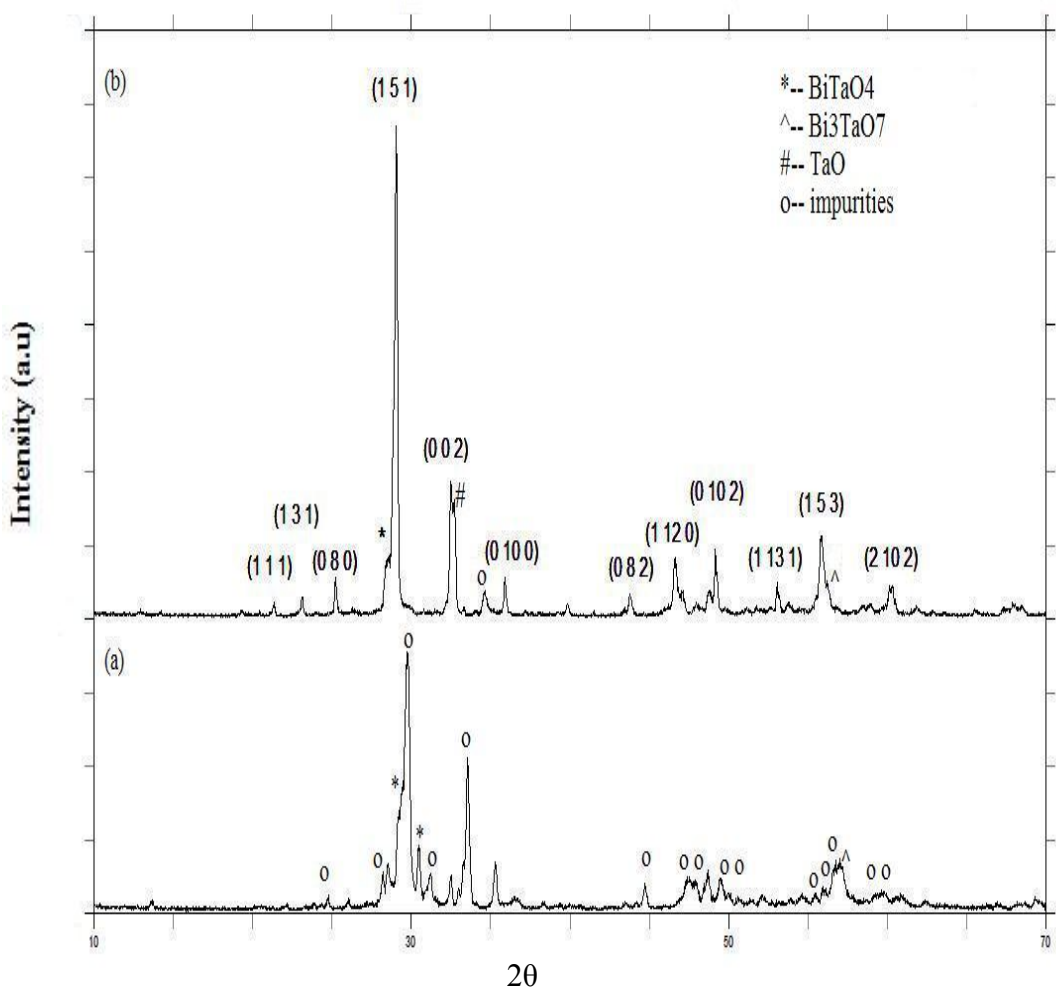


Figure 4.6 X-Ray diffraction pattern for $\text{Sr}_{0.8}\text{Bi}_{2.4}\text{Ta}_2\text{O}_9$ when it was heated at (a) 1000 °C for 2 hours and (b) 1100 °C for 4 hours.

4.1.5 Phase Formation Study of $\text{Sr}_{0.7}\text{Bi}_{2.2}\text{Ta}_2\text{O}_9$ (Solid-state Method)

Figure 4.7 shows the XRD patterns for $\text{Sr}_{0.7}\text{Bi}_{2.2}\text{Ta}_2\text{O}_9$ synthesized at (a) 1000 °C for 2 hours (b) 1100 °C for 4 hours. From the pattern, it can be seen that when the compound was heated at 1000 °C for 2 hours, there were many impurity peaks existed that indicated it required further higher and longer heat treatment. When it is further heat to 1100 °C for 4 hours, it enhanced the crystallinity and impurity peaks are reduced. The impurity peaks are mainly formed by BiTaO_4 and Bi_3TaO_7 . The refined lattice parameters are $a = 5.5392 \text{ \AA}$, $b = 25.117 \text{ \AA}$ and $c = 5.5257 \text{ \AA}$, $\alpha = \beta = \gamma = 90^\circ$, respectively.

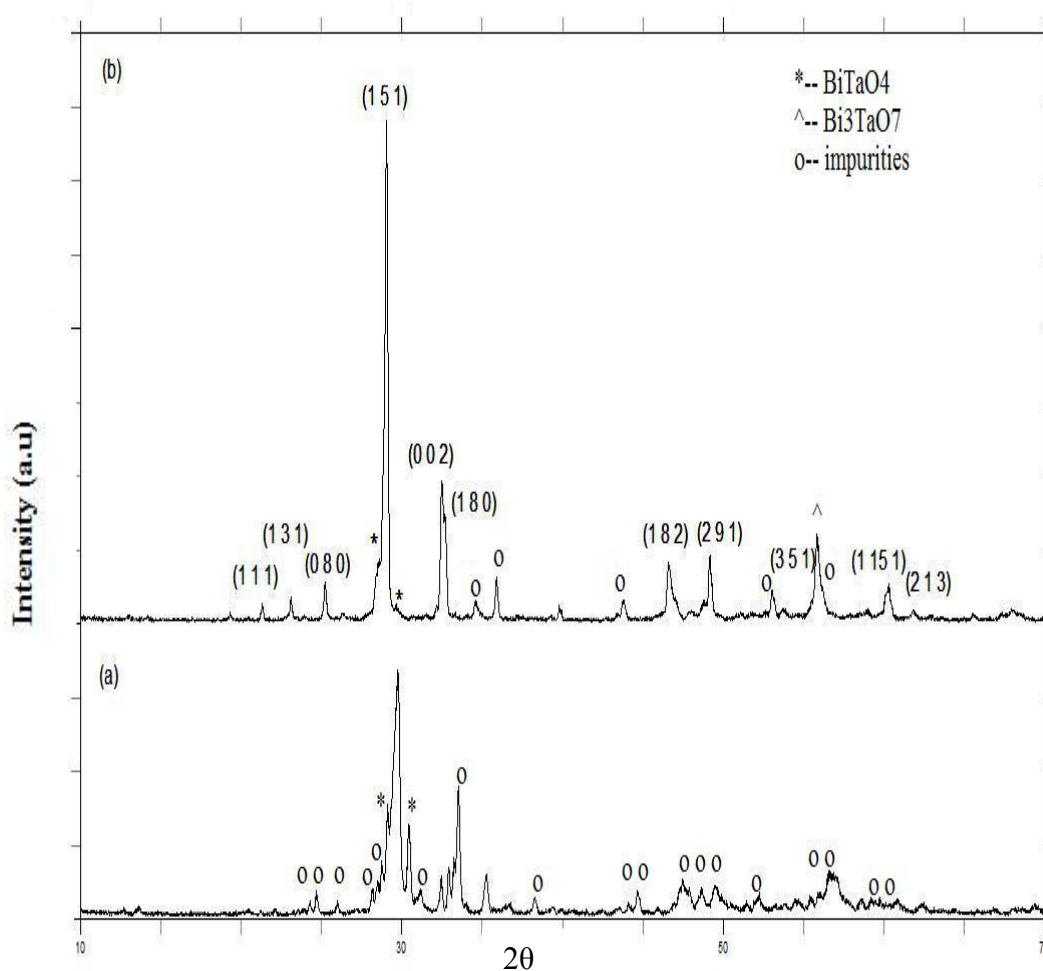


Figure 4.7 X-Ray diffraction pattern for $\text{Sr}_{0.7}\text{Bi}_{2.2}\text{Ta}_2\text{O}_9$ synthesized at (a) 1000 °C for 2 hours (b) 1100 °C for 4 hours.

4.1.6 Phase Formation Study of $\text{Sr}_{0.7}\text{Bi}_{2.2}\text{Ta}_2\text{O}_9$ (Ball Milling)

Figure 4.8 shows XRD patterns of $\text{Sr}_{0.7}\text{Bi}_{2.2}\text{Ta}_2\text{O}_9$ which undergoes ball milling process for 4 hours then heated at (a) 850 °C for 4 hours and (b) 950 °C for 4 hours. After heated for 4 hours at 950 °C, the crystallinity of the compound was enhanced and impurity peaks intensity was reduced. There were many impurity peaks that can be observed from the XRD pattern that involved BiTaO_4 . The refined lattice parameters were $a = 5.5736 \text{ \AA}$, $b = 25.0058 \text{ \AA}$ and $c = 5.4997 \text{ \AA}$, $\alpha = \beta = \gamma = 90^\circ$, respectively.

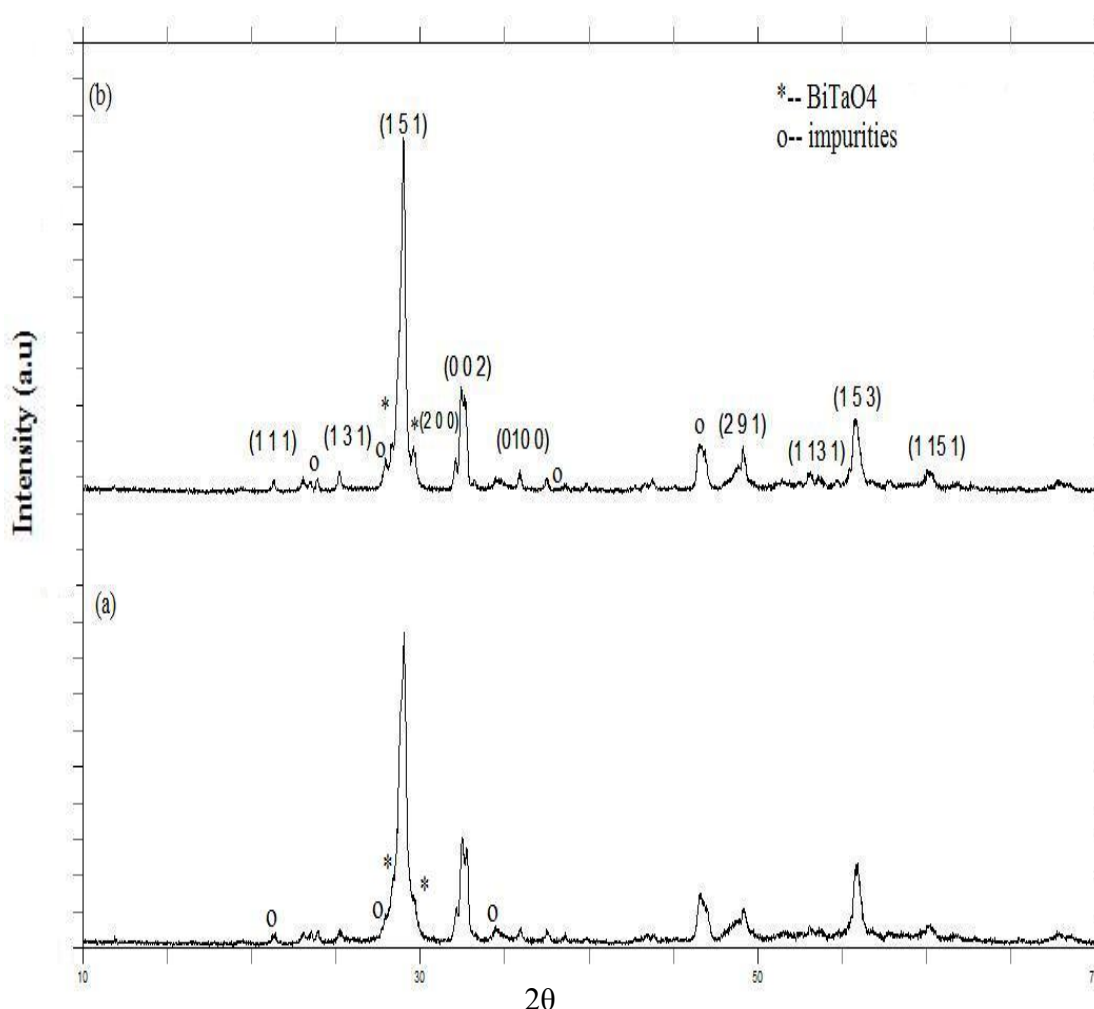


Figure 4.8 XRD pattern of $\text{Sr}_{0.7}\text{Bi}_{2.2}\text{Ta}_2\text{O}_9$ which undergoes ball milling process for 4 hours then heated at (a) 850 °C for 4 hours and (b) 950 °C for 4 hours.

4.2 Electrical Properties

AC impedance analyses were conducted to separate the possible contribution of grains and grain boundaries. Impedance analysis was performed on $\text{SrBi}_2\text{Ta}_2\text{O}_9$ with different preparation methods and $\text{Sr}_{0.9}\text{Bi}_{2.1}\text{Ta}_2\text{O}_9$ in the following sections prepared by conventional method. The result will be discussed.

4.2.1 Complex Impedance Study

A schematics model of $\text{SrBi}_2\text{Ta}_2\text{O}_9$ ceramics is described by the equivalent circuit shown in Figure 4.9. The circuit consists of two sub-circuit connected in series, one represent grains and another represent grain boundary phase. In each sub-circuit, it composed of one resistor and one capacitor parallel to each other (Wu et al., 2001). The impedance of such equivalent circuit can be described by both real part (Z') and imaginary part (Z'') with formula $Z^* = Z' + jZ''$.

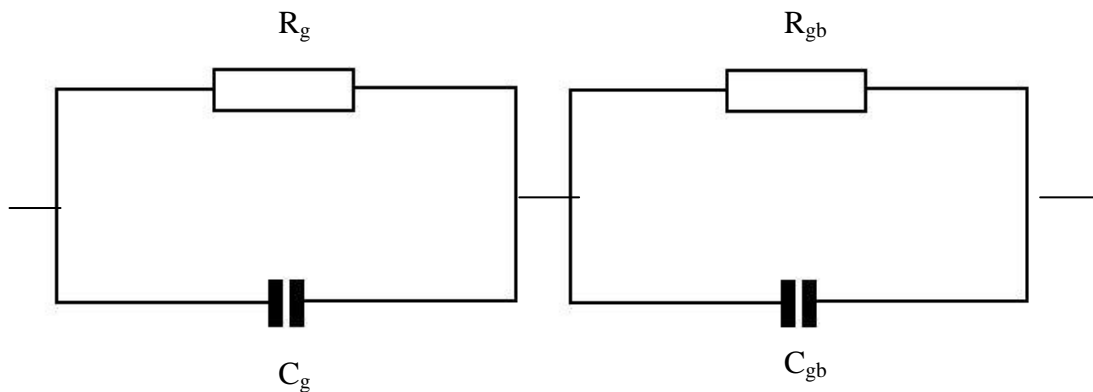


Figure 4.9 Equivalent circuits of $\text{SrBi}_2\text{Ta}_2\text{O}_9$ ceramics.

Figures 4.10, 4.11 and 4.12 show the typical impedance data Cole-cole plots of three measured samples at different temperatures. Two overlapping semicircles are seen in each figure; the high frequency arc corresponds to bulk region and low frequency arc corresponds to grains boundary. The results show that there is a decrease in resistance that may be associated with bulk/grain boundary region of the sample when the temperature of measurement increased.

Wu et al. (2001) reported that there are mainly two overlapping semicircles in $\text{SrBi}_2\text{Ta}_2\text{O}_9$ sample when it was heated below 450 °C but when the temperature was above 450 °C, three overlapping semicircles was observed. The lowest frequency range arc was attributed to be the ferroelectric-electrode interface effect (Wu et al., 2001). Existing of this low frequency range arc indicated that $\text{SrBi}_2\text{Ta}_2\text{O}_9$ is an ionic conductor; ionic carrier could be blocked at the interfaces due to the microstructural defects such as grain boundary, cracks and pores. However, in current study, only two overlapping semicircles being obtained at 700 °C for all the three samples. This may due to blocker pore size effect as mentioned in the study of Dhak, Dhak and Pramanik (2007) literature. If the blocker pore size is greater than 1 μm , it would lead to the overlapping of the semicircles. This is to be confirmed by SEM.

Capacitance values for the three samples at 700 °C at 10 kHz are shown in Table 4.1. The values are different to those reported in literature, where bulk/ grain capacitance for $\text{SrBi}_2\text{Ta}_2\text{O}_9$ at 700 °C is 126 pF and grain boundary capacitance is 4.9 nF (Wu et al., 2001). The higher capacities values in this study is probably due to the amount of impurity phases in those samples; the larger the amount, the higher the capacitance values. Hences, $\text{SrBi}_2\text{Ta}_2\text{O}_9$ prepared by ball milling with large amount of impurities (Figure 4.4) leads to the extremely high capacitance values.

Table 4.1 Capacitance of $\text{SrBi}_2\text{Ta}_2\text{O}_9$ measured at 700 °C at 10 kHz.

Capacitance	$\text{SrBi}_2\text{Ta}_2\text{O}_9$ (conventional solid state method)	$\text{SrBi}_2\text{Ta}_2\text{O}_9$ (ball milling process)	$\text{Sr}_{0.9}\text{Bi}_{2.1}\text{Ta}_2\text{O}_9$ (conventional solid state method)
Grain, C_g	238 pF	536 pF	313 pF
Grain Boundary, C_{gb}	1.05 nF	67.7 nF	4.21 nF

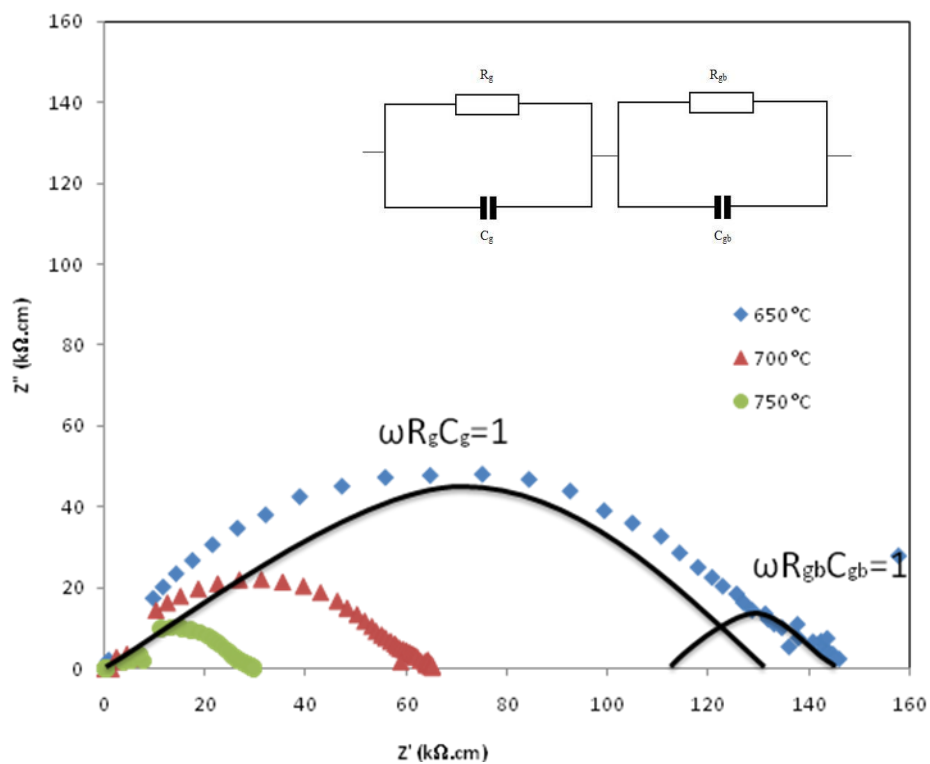


Figure 4.10 Cole-cole plot of $\text{SrBi}_2\text{Ta}_2\text{O}_9$ (solid state method) at 650 °C, 700 °C and 750 °C.

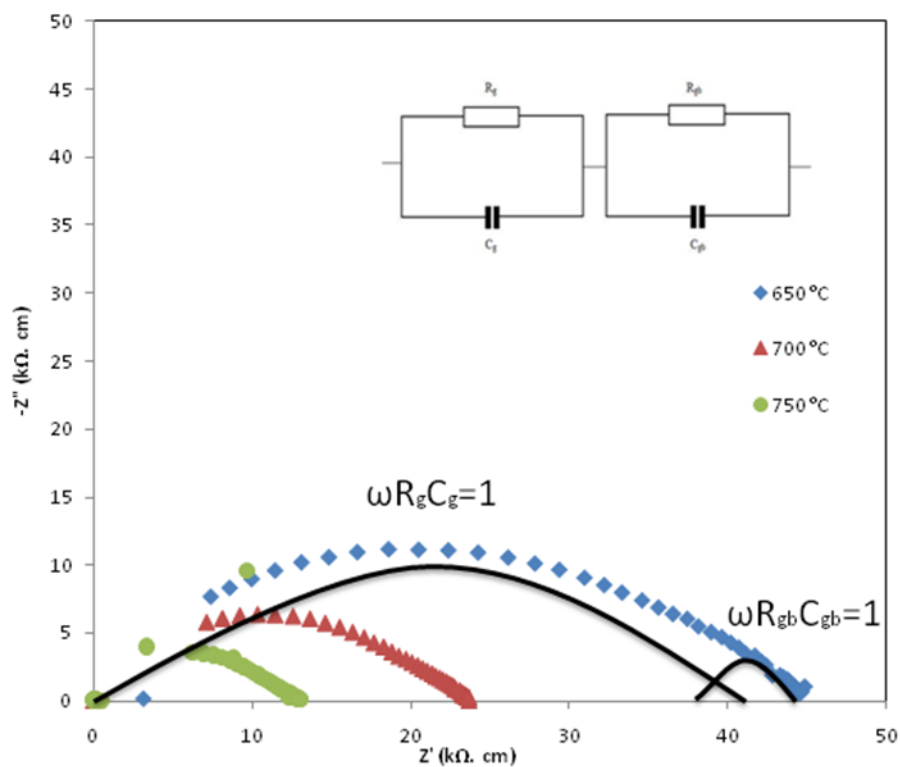


Figure 4.11 Cole-cole plot of $\text{SrBi}_2\text{Ta}_2\text{O}_9$ (ball milling) at 650 °C, 700 °C and 750 °C.

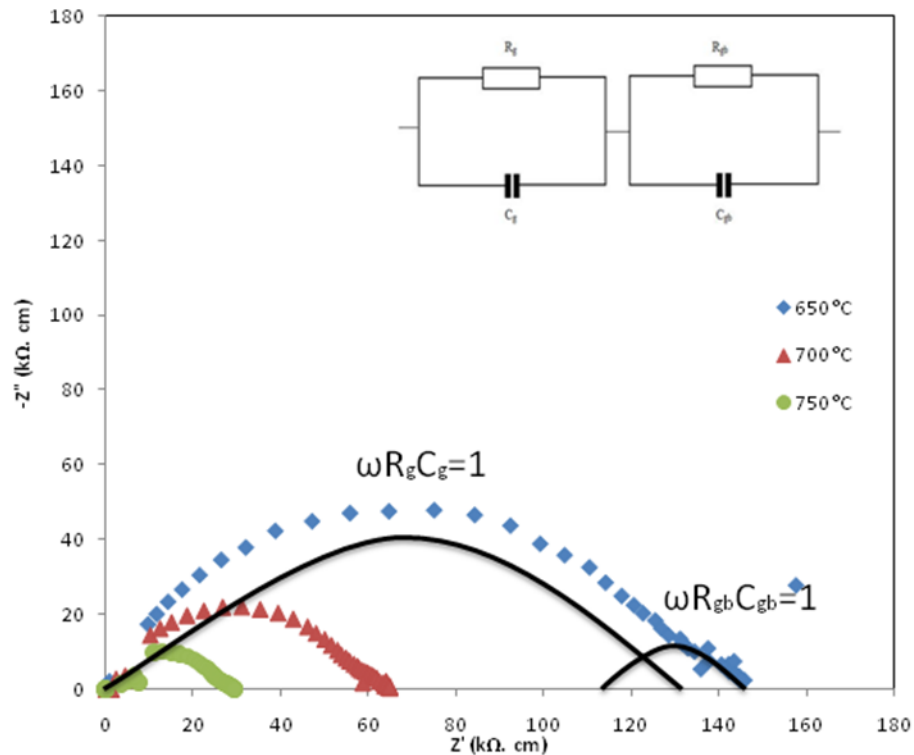


Figure 4.12 Cole-cole plot of $\text{Sr}_{0.9}\text{Bi}_{2.1}\text{Ta}_2\text{O}_9$ (solid state method) at 650 °C, 700 °C and 750 °C.

Figures 4.13- 4.15 show two peaks of Z'' that correspond to contribution of grain (high frequency) and the grain boundary (low frequency) phases. For $\text{SrBi}_2\text{Ta}_2\text{O}_9$ prepared by conventional solid state method, the half height width of the Z'' peak is approximately 1.26 decade while for $\text{Sr}_{0.9}\text{Bi}_{2.1}\text{Ta}_2\text{O}_9$, the value is 1.05 decade. Those values are close to ideal Debye of 1.14 decade indicates that samples may be homogenous (Haffz, 2005). For $\text{SrBi}_2\text{Ta}_2\text{O}_9$ prepared by ball milling process, the half height width of the Z'' peak is 2.05 decade indicates that it is a heterogeneous material. This is due to limited milling as mention earlier.

Figures 4.16, 4.17 and 4.18 show the imaginary part of impedance, as a function of frequency for the three measured samples. Dispersion can be seen in the figure and the maxima of the curves correspond to grain phase are displaced high frequencies with the increase in measuring temperature indicates the reduction of bulk resistivity (Wu et al., 2001) and existence of a temperature dependent electrical

relaxation phenomenon in the materials. The relaxation process might be due to the presence of immobile species/electrons at low temperature and defects/vacancies at higher temperature (Dhak, Dhak & Pramanik 2007).

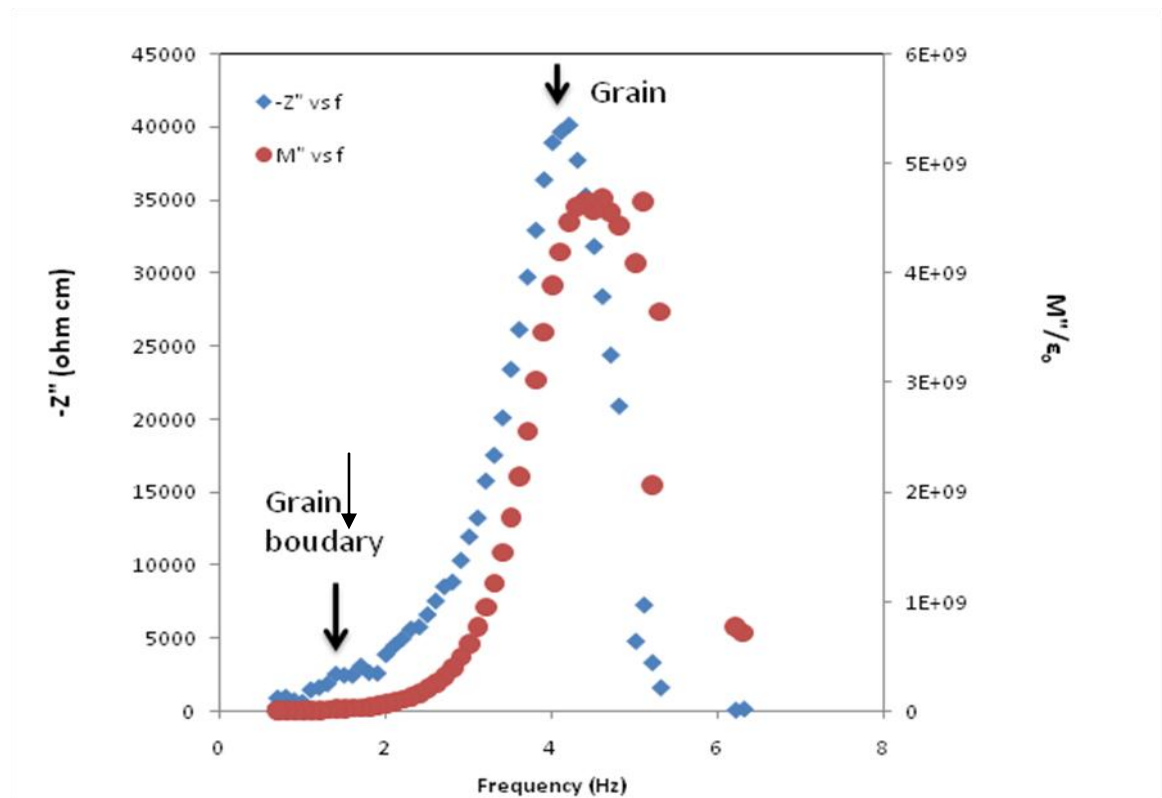


Figure 4.13 Combined spectroscopic plots of SrBi₂Ta₂O₉, prepared by conventional solid state method at 700 °C.

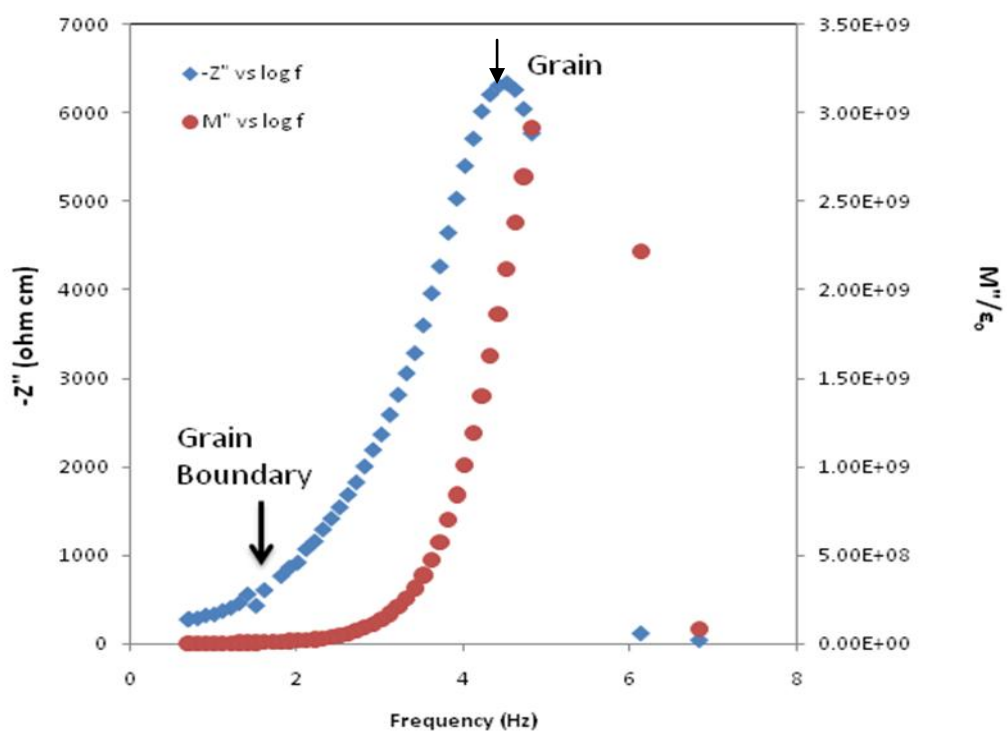


Figure 4.14 Combined spectroscopic plot of $\text{SrBi}_2\text{Ta}_2\text{O}_9$ prepared by ball milling process at $700\text{ }^\circ\text{C}$.

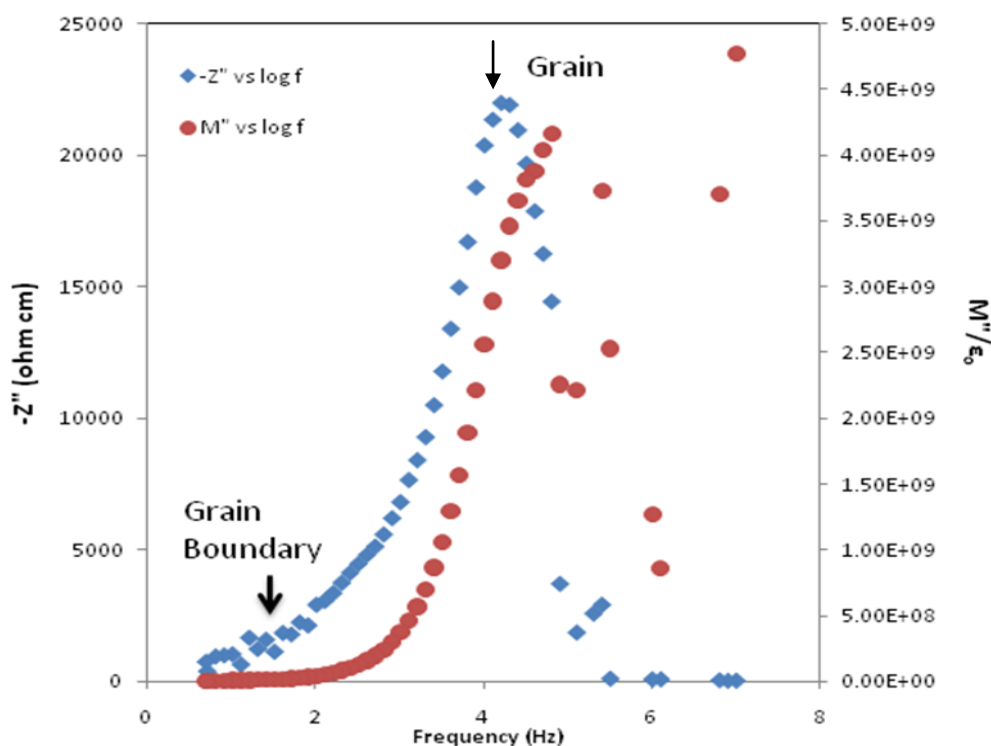


Figure 4.15 Combined spectroscopy plot for $\text{Sr}_{0.9}\text{Bi}_{2.1}\text{Ta}_2\text{O}_9$ prepared by conventional solid state method at $700\text{ }^\circ\text{C}$.

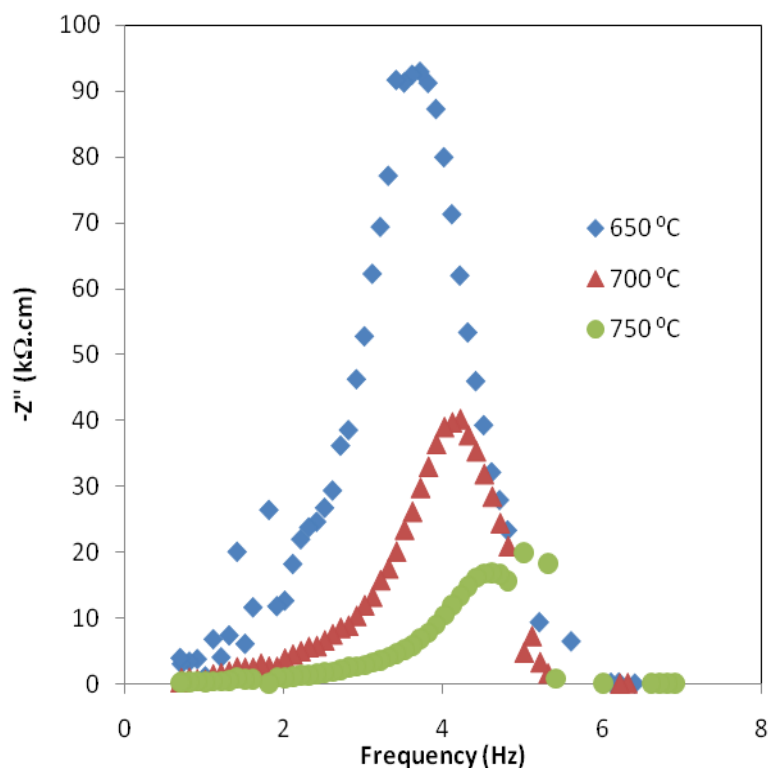


Figure 4.16 Variation of reactance Z'' with frequency at different temperatures for $\text{SrBi}_2\text{Ta}_2\text{O}_9$ prepared by conventional solid state method

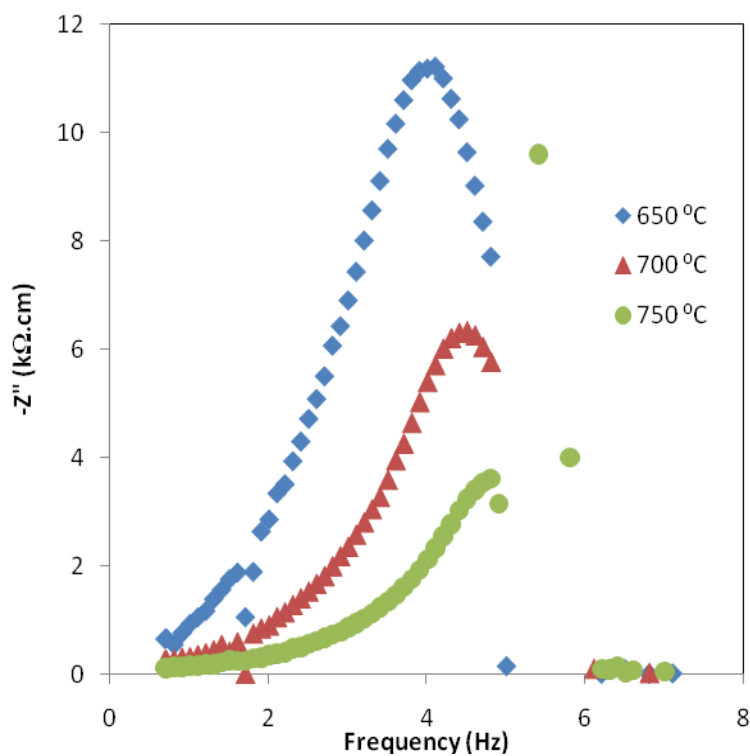


Figure 4.17 Variation of reactance Z'' with frequency at different temperatures for $\text{SrBi}_2\text{Ta}_2\text{O}_9$ prepared by ball milling process

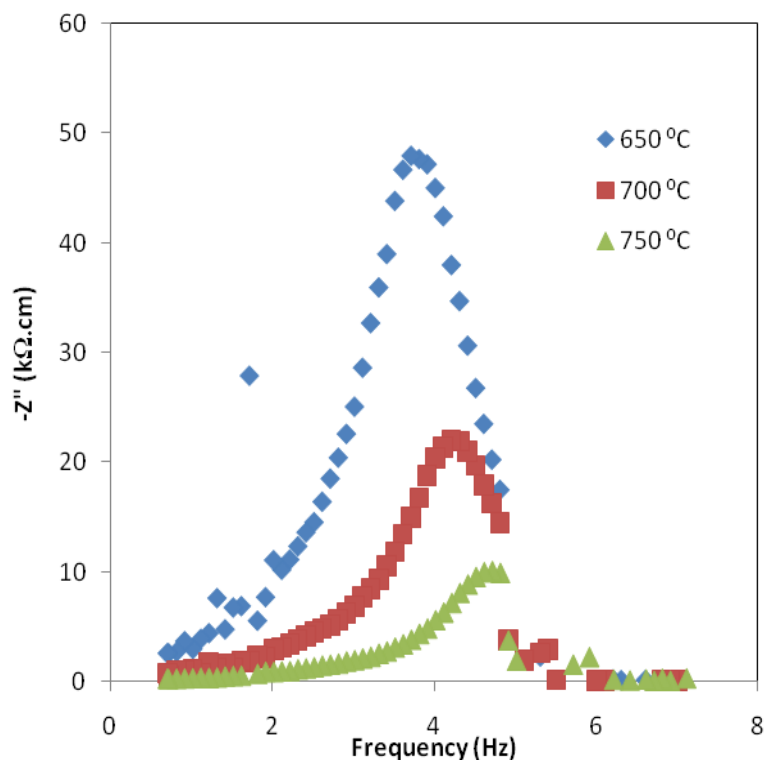


Figure 4.18 Variation of reactance Z'' with frequency at different temperatures for $\text{Sr}_{0.9}\text{Bi}_{2.1}\text{Ta}_2\text{O}_9$ prepared by conventional solid state method

4.2.2 Permittivity and Dielectric Loss Studies

Permittivity, ϵ' and dielectric loss, $\tan \delta$ of the three measured samples measured at 10 kHz are given in Table 4.2 and 4.3, respectively. Most of the application of $\text{Sr}_{1-x}\text{Bi}_{2+2x/3}\text{Ta}_2\text{O}_9$ materials are in low temperature, for example, non-volatile ferroelectric random access memory (NvFRAM) used in the computer as flash memory or Electrically Erasable Programmable Read Only Memory. Thus, only low temperature data are reported in the study.

In the study of Anderson and Roberto (2007), ϵ' for $\text{SrBi}_2\text{Ta}_2\text{O}_9$ is 260, measured at room temperature, at 10 kHz. The value of ϵ' obtained from the project for $\text{SrBi}_2\text{Ta}_2\text{O}_9$ prepared by both methods are comparable to the literature. On the other hand, the values of ϵ' for $\text{Sr}_{0.9}\text{Bi}_{2.1}\text{Ta}_2\text{O}_9$ is quite high compare to standard values obtained from literature. This is due to the presence of high intensity SrTaO_6 impurities in the sample. According to Anderson and Roberto (2007), $\tan \delta$ tends to increase with temperature particularly temperature higher than 400 °C. This could be caused by a higher concentration of charge carriers (positive and negative vacancies) at higher temperature. However, in the current study (Table 4.3), no significant trend is observed.

Table 4.2 ϵ' of $\text{Sr}_{1-x}\text{Bi}_{2+2x/3}\text{Ta}_2\text{O}_9$ (x=0, 0.1) materials measured at 10 kHz

Composition	Process method	ϵ' (28 °C)	ϵ' (100 °C)	ϵ' (200 °C)
$\text{SrBi}_2\text{Ta}_2\text{O}_9$ (x=0)	conventional solid state method	221	230	283
$\text{SrBi}_2\text{Ta}_2\text{O}_9$ (x=0)	ball milling process	275	294	407
$\text{Sr}_{0.9}\text{Bi}_{2.1}\text{Ta}_2\text{O}_9$ (x=0.1)	conventional solid state method	435	463	499

Table 4.3 $\tan \delta$ of $\text{Sr}_{1-x}\text{Bi}_{2+2x/3}\text{Ta}_2\text{O}_9$ ($x=0, 0.1$) materials measured at 10 kHz

Composition	Process method	$\tan \delta$ (28 °C)	$\tan \delta$ (100 °C)	$\tan \delta$ (200 °C)
$\text{SrBi}_2\text{Ta}_2\text{O}_9$ ($x=0$)	conventional solid state method	0.002	0.010	0.344
$\text{SrBi}_2\text{Ta}_2\text{O}_9$ ($x=0$)	ball milling process	0.014	0.062	0.0598
$\text{Sr}_{0.9}\text{Bi}_{2.1}\text{Ta}_2\text{O}_9$ ($x=0.1$)	conventional solid state method	0.055	0.004	0.011

4.2.3 Conductivity

Figures 4.19, 4.20 and 4.21 show the Arrhenius plots of the three measured samples. Conductivities of grain and grain boundary phases had been calculated from impedance at 700 °C and their corresponded activation energies are summarised in Table 4.4. Ball milled $\text{SrBi}_2\text{Ta}_2\text{O}_9$ has higher conductivity values compare to that prepared by solid state method. Conductivity increased probably because of the increase in number and mobility of charge carriers due to the formation of defects (oxygen vacancies) when the material is formed. These oxygen vacancies will be created in $\text{SrBi}_2\text{Ta}_2\text{O}_9$ by evaporation of bismuth oxide during sintering (Wu et al., 2001).

The activation energies of the three samples range between 1.17 to 1.30 eV, which in good agreement with the reported value 1.019 to 1.315 eV. Changes in chemical composition, crystallinity and microstructure would result in the change of activation energy of diffusion (Wu et al., 2001). Therefore, all the three samples should have different activation energy value. In addition, activation energy for grain boundary is always higher than that of grain for each sample. This is because

diffusion of grain boundary is smaller than grain and thus higher resistance. As the result, more energy is needed to overcome the band gap between conduction band and valence band.

Table 4.4 Conductivity and activation energy of grain and grain boundary phases.

Composition	Process method	σ for grain (700 °C)	σ for grain boundary (700 °C)	E_a (grain) (eV)	E_a (grain boundary) (eV)
SrBi₂Ta₂O₉ (x=0)	conventional solid state method	2.40 x 10 ⁻⁶	2.14 x 10 ⁻⁶	1.29	1.30
SrBi₂Ta₂O₉ (x=0)	ball milling process	1.25 x 10 ⁻⁵	1.20 x 10 ⁻⁵	1.22	1.28
Sr_{0.9}Bi_{2.1}Ta₂O₉ (x=0.1)	conventional solid state method	4.47 x 10 ⁻⁶	3.95 x 10 ⁻⁶	1.17	1.28

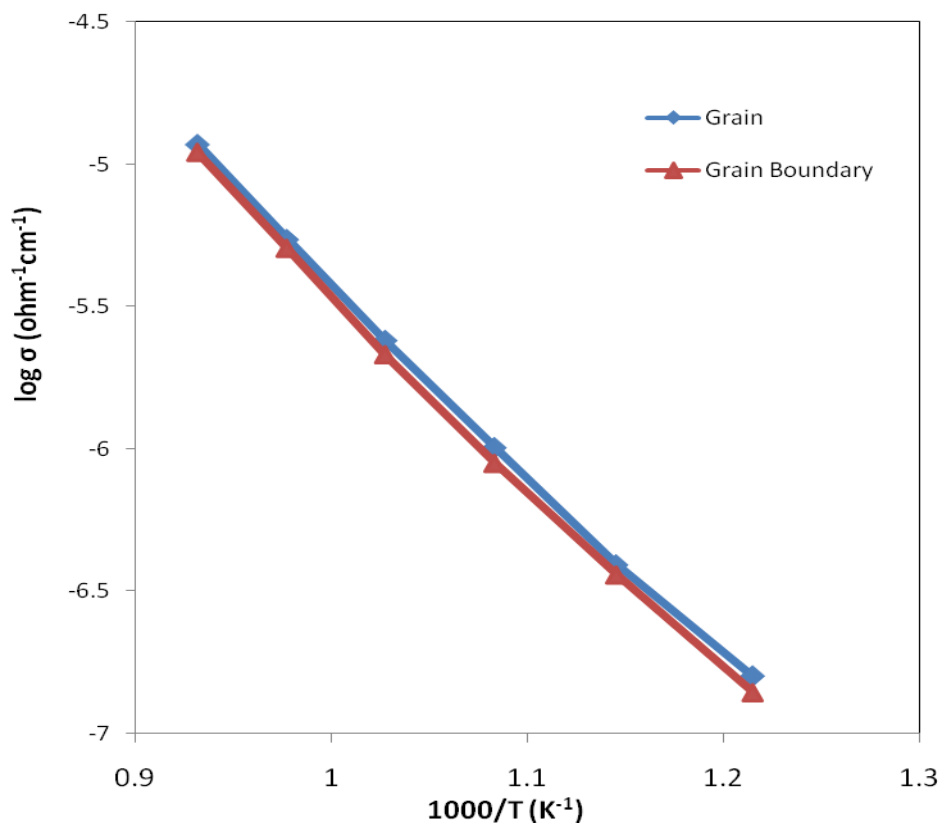


Figure 4.19 Arrhenius plot of $\text{SrBi}_2\text{Ta}_2\text{O}_9$ (solid-state method)

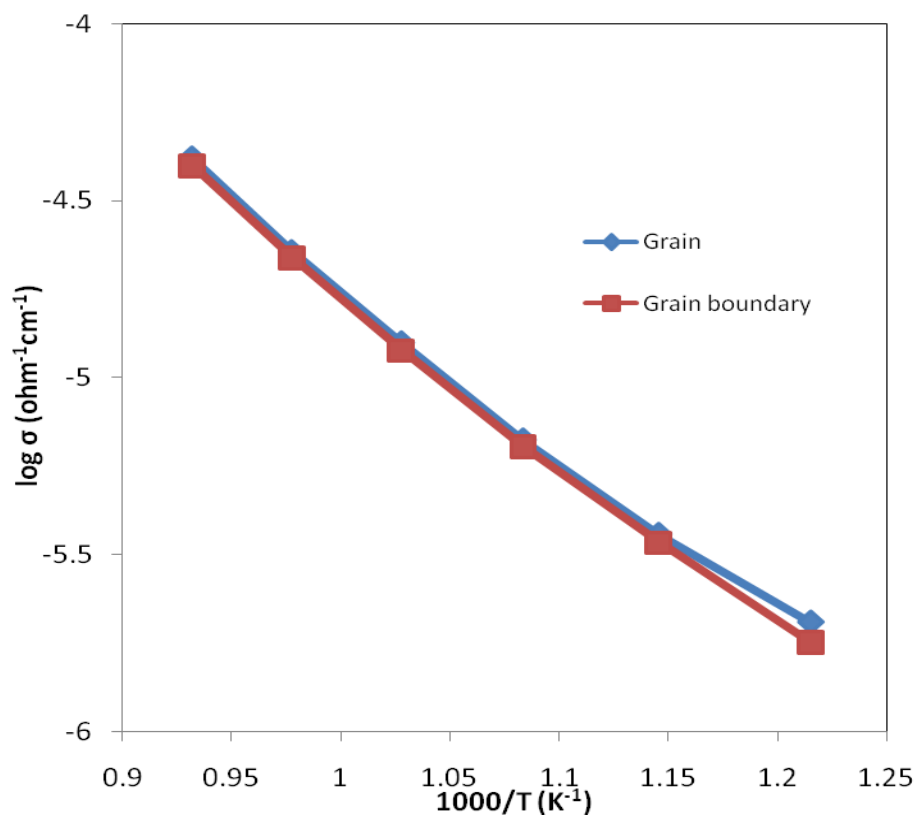


Figure 4.20 Arrhenius plot of $\text{SrBi}_2\text{Ta}_2\text{O}_9$ (ball milling)

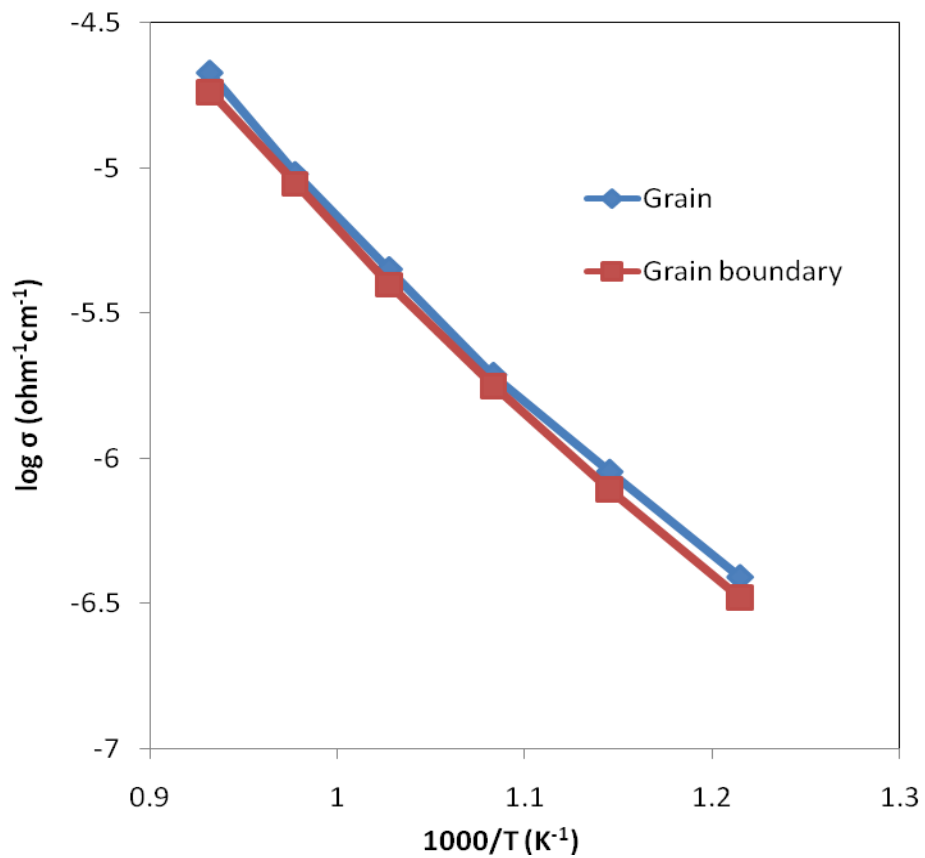


Figure 4.21 Arrhenius plot of $\text{SrBi}_2\text{Ta}_2\text{O}_9$ (solid-state method)

CHAPTER 5

CONCLUSION AND RECOMMENDATIONS

5.1 Conclusion

Two preparation processes are conventional solid state and ball milling methods used in this study. $\text{Sr}_{1-x}\text{Bi}_{2+2x/3}\text{Ta}_2\text{O}_9$ ($x= 0, 0.1, 0.2, 0.3$) powders are synthesized using solid state reaction method at 1100 °C for 4 hours while $\text{Sr}_{1-x}\text{Bi}_{2+2x/3}\text{Ta}_2\text{O}_9$ ($x= 0$ and 0.3) are synthesized by ball milling method heating time of 4 hours, at 950 °C. There are some impurity phases being observed in the samples.

The electrical measurements for three samples, $\text{SrBi}_2\text{Ta}_2\text{O}_9$ prepared by solid state and ball milling method and $\text{Sr}_{0.9}\text{Bi}_{2.1}\text{Ta}_2\text{O}_9$ by conventional method were carried out as a function of temperature and frequency. Two overlapping semicircles are seen in each figure; the high frequency arc corresponds to bulk region and low frequency arc corresponds to grains boundary. $\tan \delta$ and ϵ' measured at room temperature, 10 kHz of $\text{SrBi}_2\text{Ta}_2\text{O}_9$ ceramics are closed to those reported in the literature but are highly difference for $\text{Sr}_{0.9}\text{Bi}_{2.1}\text{Ta}_2\text{O}_9$, which may be caused by high intensity of impurities in the sample. The activation energies of the three samples, range between 1.17 to 1.30 eV in good agreement with those reported values.

5.2 Recommendation

In general, synthesis of $\text{Sr}_{1-x}\text{Bi}_{2+2x/3}\text{Ta}_2\text{O}_9$ materials can be carried out via conventional solid state reaction that involves relatively high temperature and long time of reaction which implying the possibilities for lose in stoichiometry. Besides that, uncontrollable size of powder is one of the problems. Although a better way had been used which is ball milling process, however, because of the rules and regulation in the lab which is ball milling machine cannot used overnight, thus samples is only milled for four hours. As the result, impurities in the samples cannot be fully eliminated since impurity phases can only being removed when it is milled up to 50 hours (Chew, Srinivas, Sritharan and Boey, 2005). As the result, hopefully the rules and regulation of using the equipment can be changed.

Besides using XRD analysis to determine phase purity of the samples, Scanning Electron Microscopy (SEM) and Thermogravimetric Analysis (TGA) should be carried out in this experiment. SEM produced very high resolution image of the samples and therefore, by performing the analysis, microstructural observation of sintered surface can be known. Since porosity of the surface will cause decrease in permittivity of the material, thus, it is possible to prove the reason for permittivity to reduce.

It is required to check weight loss of the sample to ensure Bi loss is still in controlled when it is undergoes sintering process. Thus, TGA is necessary and served for this purpose. TGA is means to determine changes of sample to temperature. Besides that, it can also be used to absorb moisture and estimate corrosion kinetics in high temperature oxidation.

Finally, Elemental Analysis Technique can be also used in the project which serves as the purpose to determine the weight percentage of the composition for the samples. By using this technique, composition of the samples can be determined accurately as well as determined unknown phase in the samples to help to ascertain the structure.

REFERENCES

- Asit, B. P., Abhijit, T., Amita, P., & Panchanan, P. (2004). Chemical synthesis and characterisation of nanocrystalline $ABi_2Ta_2O_9$ (A=Sr, Ba and Ca powder). *Ceramics International*, 30, 715-720 .
- Asit, B. P., Abhijit, T., & Panchanan, P. (2003). Synthesis, characterisation and properties of nano-sized SBT ceramics prepared by chemical route. *Journal of the European Ceramics Society*, 24, 3043-3048.
- Haffz, A. M., & A. H. (2005). Study of Dielectric Relaxation in Zn, Cd, and Hg, Ethanolamine Complexes. *Physics Department, Faculty of Science, Alexandria University, Alexandria, Egypt* .
- Anderson, D., & Roberto, L. M. (2007). Production of Sr-deficient bismuth tantalates from microwave-hydrothermal derived precursor: Structural and dielectric properties. *Physics and Chemistry of Solid*, 68 , 645-649.
- Chen, W., Shoichi, K., Cihangir, D., & Koji, W. (2006). Preparation of single crystalline $Sr_{0.5}Ba_{0.5}Nb_2O_6$ particles . *Journal of the European Ceramics Society* 26, 647-653.
- Chew, C. L., Srinivas, A., Sritharan, T., & Boey, F. Y. C. (2005). Mechanochemical activation of strontium bismuth tantalate synthesis. *Scripta Materialia*, 53, 1197-1199 .
- Choong, H. F. (2010). Synthesis and Characterisation of Dielectric Material.
- Chou, H. Y., Chen, T. M., & Tseng, T. Y. (2003). Electrical and dielectric properties of low-temperature crystallized SBT thin films on Ir/SiO₂/Si substrates. *Materials chemistry and physics*, 82, 826-830.
- Chie, F., Rintaro, A., Hiraoki, T., Soichiro, O., & Tadashi, S. (2005). Effect of non-stoichiometric on ferroelectricity and piezoelectricity in strontium bismuth tantalate ceramics. *Journal of European Ceramics Society*, 25, 2723-2726 .
- Dhak, D., Dhak, P., & Pramanik, P. (2007). Influence of substitution on dielectric and impedance spectroscopy of $Sr_{1-x}Bi_{2+y}Nb_2O_9$ ferroelectric ceramics synthesized by chemical route. *Applied Surface Science*, 254, 3078-3092.

- Dhak, D., Biawas, S. K., & Pramanik, P. (2006). Synthesis and characterisation of nanocrystalline $\text{SrBi}_2\text{Nb}_2\text{O}_9$ ferroelectric ceramics using TEA as the polymeric matrix. *Journal of the European Ceramics Society*, 26, 3717-3723 .
- Nelis, D., Vanhoyland, A., Van Werde, H., et al. (2005). Synthesis of strontium bismuth niobate ($\text{SrBi}_2\text{Nb}_2\text{O}_9$) using an aqueous acetate-citrate precursor gel: thermal decomposition and phase formation. *Thermochimica Acta*, 426, 39-48.
- Jha, G., Roy, A., Dhar, A., Mannar, I., & Ray, S. K. (2007). Effect of annealing temperature on the structural and electrical properties of $\text{SrBi}_2\text{Ta}_2\text{O}_9$ thin film for memory-based application . *Physics B*, 400, 33-37
- Gao, J., Erjia, L., Zhibin, Z., Jianqing, C., & Aiping, Z. (2003). Structure of post-annealed ferroelectric $\text{PbZr}_x\text{Ti}_{1-x}\text{O}_3$ and $\text{SrBi}_2\text{Ta}_2\text{O}_9$ thin films . *Thin solid films*, 424, 79-83 .
- Huang, C. H., Chou, H. Y., Lian, C. W., & Tseng, T. Y. (2004). Electrical and dielectric behavior of fluorite-like SBT thin film pyrolyzed and thermally annealed at 450 °C . *Materials Chemistry and Physics*, 83, 345-349.
- Li, B., Li, L., & Wang, X. (2002). Sintering behavior of bulk SBT prepared by solid state reaction . *Ceramics International*, 29, 351-353.
- Lu, C. H., & Lee, J. T. (1998). Strontium Bismuth Tantalate Layered Ferroelectric Ceramics: Reaction Kinetics and Thermal Stability . *Ceramics International*, 24, 285-291.
- Rajni, J., Vinay, G., Abhai, M., & Sreenivas, K. (2004). Ferroelectric and piezoelectric properties of non-stoichiometric $\text{Sr}_{1-x}\text{Bi}_{2+2x/3}\text{Ta}_2\text{O}_9$ ceramics prepared from sol-gel derived powders *Materials science and engineering B*, 112, 54-58 .
- O'Brien, S., Crean, G. M., Cakare, L., & Kosec, M. (2005). Structural and electrical characterisation of strontium bismuth tantalate (SBT) thin film. *Applied Surface Science*, 252, 4497-4501.
- Sritharan, T., Boey, F. Y. C., & Srinivas, A. (2007). Synthesis of complex ceramics by mechanochemical activation, *Journal of Materials Processing Technology*, 192-2193, 255-258 .
- Wu, Y., Mike, J. F., Seana, S., Steven, J. L., Tammy, P. C., & Guozhong, C. (2001). Impedance study of $\text{SrBi}_2\text{Ta}_2\text{O}_9$ and $\text{SrBi}_2(\text{Ta}_{0.9}\text{V}_{0.1})_2\text{O}_9$ ferroelectrics. *Material Science and Engineering*, B86, 70-78
- Yang, P., Shi, M., Qin, S., & Deng, H. (2006). Optical and electrical properties of strontium bismuth tantalate thin film . *Materials Letters*, 61, 2687-2691.
- Zanetti, E. L., Bulhoes, J. A., Leite, & E. (2003). Preparation and characterisation of nanosized $\text{SrBi}_2\text{Nb}_2\text{O}_9$ powder by the combustion analysis . *Materials Letters*, 57, 2812-2816.

Zanetti, J. S., Vasconcelos, E. R., Longo, & J. A. (2004). Low temperature crystallization of SBT thin films using microwave oven . *Thin Solid Films*, 466, 62-68.

ICDD File Number: 00-051-1683, 00-044-0202, 00-027-0050, 00-016-0906, 01-070-7771, 01-070-0248.

APPENDICES



Carbolite furnace



Pressing machine



Solartron impedance analyzer



Milling Machine



Pellet Die



Agate mortar



Bottle used for ball milling



Zirconia ball